



1 **Wetlands inform how climate extremes influence surface water expansion and contraction**

2

3 Melanie K. Vanderhoof<sup>1\*</sup>, Charles R. Lane<sup>2</sup>, Michael G. McManus<sup>3</sup>, Laurie C. Alexander<sup>4</sup>, Jay  
4 R. Christensen<sup>5</sup>

5

6 <sup>1</sup>U.S. Geological Survey, Geosciences and Environmental Change Science Center, P.O. Box  
7 25046, DFC, MS980, Denver, CO 80225

8 \*email: [mvanderhoof@usgs.gov](mailto:mvanderhoof@usgs.gov), phone: 303-236-1411

9 <sup>2</sup>U.S. Environmental Protection Agency, Office of Research and Development, National  
10 Exposure Research Laboratory, 26 W. Martin Luther King Dr., MS-642, Cincinnati, OH 45268

11 <sup>3</sup>U.S. Environmental Protection Agency, Office of Research and Development, National Center  
12 for Environmental Assessment, 26 W. Martin Luther King Dr., MS-A110, Cincinnati, OH 45268

13 <sup>4</sup>U.S. Environmental Protection Agency, Office of Research and Development, National Center  
14 for Environmental Assessment, 1200 Pennsylvania Ave. NW (8623-P), Washington, DC 20460

15 <sup>5</sup>U.S. Environmental Protection Agency, Office of Research and Development, National  
16 Exposure Research Laboratory, Environmental Science Division, 944 E. Harmon Ave., Las  
17 Vegas, NV 89119

18

19 **Abstract**

20 Effective monitoring and prediction of flood and drought events requires an improved  
21 understanding of how and why surface-water expansion and contraction in response to climate  
22 varies across space. This paper sought to (1) quantify how interannual patterns of surface-water  
23 expansion and contraction vary spatially across the Prairie Pothole Region (PPR) and adjacent  
24 Northern Prairie (NP) in the United States, and (2) explore how landscape characteristics  
25 influence the relationship between climate inputs and surface-water dynamics. Due to differences  
26 in glacial history, the PPR and NP show distinct patterns in regards to drainage development and  
27 wetland density, together providing a diversity of conditions to examine surface-water dynamics.  
28 We used Landsat imagery to characterize variability in surface-water extent across eleven  
29 Landsat path/rows representing the PPR and NP (images spanned 1985-2015). The PPR not only  
30 experienced a 2.6-fold greater surface-water extent under median conditions relative to the NP,  
31 but also showed a 3.4-fold greater change in surface-water extent between drought and deluge  
32 conditions. The relationship between surface-water extent and accumulated water availability



33 (precipitation minus potential evapotranspiration) was quantified per watershed and statistically  
34 related to variables representing hydrology-related landscape characteristics (e.g., infiltration  
35 capacity, surface storage capacity, stream density). To investigate the influence stream-  
36 connectivity has on the rate at which surface water leaves a given location, we modeled stream-  
37 connected and stream-disconnected surface water separately. Stream-connected surface water  
38 showed a greater expansion with wetter climatic conditions in landscapes with greater total  
39 wetland area. Disconnected surface water showed a greater expansion with wetter climatic  
40 conditions in landscapes with higher wetland density, lower infiltration and less anthropogenic  
41 drainage. From these findings, we can expect that shifts in precipitation and evaporative demand  
42 will have uneven effects on surface-water quantity. Accurate predictions regarding the effect of  
43 climate change on surface-water quantity will require consideration of hydrology-related  
44 landscape characteristics including wetlands.

45

#### 46 **Keywords**

47 Drought, evapotranspiration, Landsat, prairie pothole region, precipitation, surface water

48

#### 49 **1. Introduction**

50 Surface-water dynamics have strong implications for ecosystem functioning and human  
51 land use including biogeochemical balances (Hoffmann et al., 2009), species distribution  
52 (Boschilia et al., 2008; Calhoun et al., 2017), hydrologic connectivity (Heiler et al., 1995;  
53 Pringle, 2001)), and agricultural productivity (Mokrech et al., 2008; Gornall et al., 2010). Yet  
54 natural variability in surface-water extent poses a basic challenge to gathering timely, accurate  
55 information (Poff et al., 1997; Beerli and Phillips, 2007). While satellite imagery can be used to



56 map variability in surface-water extent over time, predicting future changes in surface-water  
57 extent (e.g., in response to changes in climate, land use, or natural disasters) requires improving  
58 our understanding of how the landscape influences surface-water extent over time and space. The  
59 relative importance of hydrologic processes and flowpaths across a landscape (e.g., surface  
60 storage, infiltration, evapotranspiration, runoff) can be expected to influence the timing, duration  
61 and extent of surface water for a given location (Euliss and Mushet, 1996; LaBaugh et al., 1996,  
62 van der Kamp et al., 1999)

63 Winter (2001) presented the concept of hydrologic landscapes as a means to classify  
64 landscape units based on their hydrologic attributes (land-surface form, geology and climate).  
65 These attributes, it is argued, could then be used to predict the partitioning of water into storage,  
66 infiltration, evapotranspiration and runoff (Wagener et al., 2007). In many landscapes storage is  
67 minimal and when rainfall intensity is greater than both the rate of soil infiltration and the soil  
68 moisture deficit, runoff via overland and subsurface flows will dominate, contributing to  
69 increased stream discharge (Eamus et al., 2006). These landscapes could be described as  
70 exhibiting a low potential for surface-water expansion. Alternatively, in landscapes with low  
71 topographic gradients and poorly developed drainage networks, runoff events rarely deplete  
72 available surface storage, meaning that although stream discharge may elevate, much of the  
73 surplus water remains as surface water (Shaw et al., 2012; Kuppel et al., 2015). These landscapes  
74 show a high potential for surface-water expansion with evapotranspiration often the primary  
75 mechanism for water loss (Winter and Rosenberry, 1998). Landscapes with a tendency to  
76 accumulate surface-water are relatively common across the globe and include former glacial  
77 landscapes including the Prairie Pothole Region (PPR) (Sass and Creed, 2008; Shaw et al.,  
78 2012), and parts of China (Yao et al., 2007) and Russia (Stokes et al., 2007), permafrost regions



79 (Smith et al., 2007), as well as low gradient landscapes including the Argentine Pampas (Kuppel  
80 et al., 2015); the Pantanal in Brazil (Hamilton, 2002), and the Orinoco Llanos in Columbia and  
81 Venezuela (Hamilton, 2004). Although such landscapes have previously been shown to  
82 experience surface-water expansion in response to increased precipitation (Huang et al., 2011;  
83 Kuppel et al., 2015; Vanderhoof et al., 2016) or melting ice (Stokes et al., 2007; Yao et al.,  
84 2007), we are unaware of studies that have explicitly compared surface-water expansion and  
85 contraction between landscapes of differing surface-water expansion potential.

86 The PPR and adjacent Northern Prairie (NP), which span the upper mid-west of the  
87 United States, occur within and beyond the last glacial maximum, respectively, and together  
88 represent a range in the potential for surface-water expansion. The PPR is characterized by a  
89 high density of depressional wetland and lake features (Zhang et al., 2009), a relic of glacial  
90 retreat (Flint, 1971). Most wetlands are relatively small (< 0.5 ha) depressions, underlain by  
91 glacial till with low permeability, and occur within a landscape matrix of natural grassland and  
92 agriculture (Winter and Rosenberry, 1995; Zhang et al., 2009; Cohen et al., 2016). This is in  
93 contrast to the adjacent NP such as the Northwestern Great Plains (Montana, western North and  
94 South Dakota) and the Central Irregular Plains (southern Iowa and northern Missouri), which  
95 lack the high density of small wetlands and show a well-developed drainage network due to its  
96 occurrence outside of the last maximum glacial extent (USGS, 2013). The NP and PPR are also  
97 characterized by substantial spatial and interannual variability in air temperature and  
98 precipitation (Bryson and Hare 1974). Variations in temperature and moisture content of  
99 competing air masses results in a strong north-south temperature and east-west precipitation  
100 gradient. The precipitation-evaporation deficit is least in the east (i.e., Minnesota and Iowa), and  
101 increases to the west (i.e., Montana) (Kantrud et al., 1989; Millet et al., 2009). This variability in



102 climate has a strong influence on water levels across the region. In the PPR in spring, wetland  
103 depressions receive water from both precipitation and snowmelt. In the summer, water level is  
104 controlled by direct precipitation, evaporation and wetland vegetation transpiration (Winter and  
105 Rosenberry, 1995; LaBaugh et al., 1998; Carroll et al., 2005), with evapotranspiration typically  
106 dominating water loss (Rosenberry et al., 2004).

107 Monitoring variation in water levels across the PPR has been of high interest as it is a key  
108 factor in flood abatement, water quality, biodiversity, carbon management and aquifer recharge  
109 (Gleason et al., 2008). Water level data at Devils Lake, North Dakota, for example, have been  
110 collected as far back as 1867 and provide a regional indicator of hydrological conditions (Wiche,  
111 1996; LaBaugh et al., 1996). Efforts have been expanded to map interannual changes in surface-  
112 water extent across the PPR at a landscape scale using remotely sensed imagery (Kahara et al.,  
113 2009; Niemuth et al., 2010; Vanderhoof et al., 2016). However, while substantial interannual  
114 variation in water level has been documented across the PPR (Huang et al., 2011; Vanderhoof et  
115 al., 2016), and primarily attributed to interannual variation in temperature and precipitation  
116 (Johnson et al., 2005; Zhang et al., 2009), such surface-water patterns have to date been  
117 minimally characterized for the remainder of the NP. In addition to interannual patterns of  
118 temperature and precipitation, we would also expect that surface-water extent will depend on  
119 landscape parameters such as infiltration capacity, storage capacity, and drainage characteristics  
120 (Euliss and Mushet, 1996; LaBaugh et al., 1996; van der Kamp et al., 1999). Spatial models  
121 incorporating some of these factors can provide additional insights into the risk of flood and  
122 drought events across the PPR (Niemuth et al., 2010).

123 The PPR, in conjunction with adjacent NP, provides an ideal physiographic example in  
124 which to analyze the influence of landscape characteristics on surface-water expansion and



125 contraction. Although the interaction between water level and climate has been studied  
126 extensively at select locations within the PPR (e.g., Cottonwood Lake) (Winter and Rosenberry,  
127 1998; Huang et al. 2011), minimal research has sought to understand spatial variability in the  
128 relationship between climate and surface-water extent. Our research questions addressed in this  
129 study are:

130 (1) How do interannual patterns of surface-water expansion and contraction vary  
131 spatially across the Prairie Pothole Region and adjacent Northern Prairie of the  
132 United States?

133 (2) How do landscape characteristics influence the relationship between climate inputs  
134 and surface-water dynamics?

135 The successful exploration of this spatial patterning and landscape-scale statistical functions will  
136 inform hydrologic/hydraulic and biogeochemical modeling and has implications for  
137 biodiversity/habitat modeling and management (e.g., Allen et al., 2016; Golden et al., 2017)

## 138 **2. Methods**

139 As detailed below, we used Landsat imagery to map surface-water extent under dry,  
140 average, and wet conditions across portions of the PPR and adjacent NP. We compared the  
141 expansion and contraction of surface-water extent between the PPR and adjacent NP. As stream-  
142 connected surface water can leave a location easily as stream flow, stream-connected and  
143 disconnected surface water were analyzed separately. We then used a two-level modeling  
144 approach to investigate the influence of landscape variables on surface-water dynamics. In the  
145 first stage, surface-water extent per watershed was statistically related to accumulated water  
146 availability, defined as precipitation minus potential evapotranspiration. This first stage produced  
147 the dependent variable for the second model, the slope of the relationship between surface-water



148 extent and climate inputs per hydrological unit (a watershed) or the Surface Water Climate  
149 Response (SWCR). The SWCR was then regressed against independent variables representing  
150 landscape characteristics (e.g., infiltration capacity, surface storage capacity, stream density,  
151 long-term climate normals). This approach allowed us to explore what landscape characteristics  
152 drive spatial variability in the relationship between surface-water extent and climate.

153

## 154 **2.1 Study Area**

155 Our study area consisted of eleven Landsat path/rows (total area = 308,439 km<sup>2</sup>) in the  
156 U.S. portion of the PPR and adjacent NP (Figure 1). The PPR across North and South Dakota,  
157 western Minnesota, northern Iowa and northern Nebraska, is dominated by the North and  
158 Northwest Glaciated Plains. This ecoregion is characterized by landscape features formed during  
159 its recent glacial history. Drift plains, large glacial lake basins and shallow river valleys support  
160 row crop agriculture. Grasslands and livestock grazing dominate areas where glaciers left  
161 deposits of uneven glacial till (Sayler et al., 2015). The PPR is dominated by cultivated crops  
162 (59%), herbaceous (18%) and hay/pasture (10%) (Homer et al., 2015). Adjacent to the PPR, the  
163 Northwestern Great Plains, across western North and South Dakota, is a semiarid unglaciated  
164 plain which tends to have shallow soils with a clay texture not conducive to growing crops and  
165 instead dominated by livestock grazing across grasslands (Sayler et al., 2015). To the southeast  
166 of the North Glaciated Plains lies the Western Corn Belt and the Central Irregular Plains in Iowa  
167 and Nebraska. Glacial till forms the parent material for most of the soil in Western Corn Belt and  
168 the northern part of the Central Irregular Plains, within the study area. Level and gently rolling  
169 hills and fertile soils support agriculture (Sayler et al., 2015). The NP is dominated by  
170 herbaceous land cover (47%) with cultivated crops (28%) and hay/pasture (9%) is also common



171 (Homer et al., 2015). Using the precipitation averages (1981-2010) defined by the Parameter-  
172 elevation Regressions on Independent Slopes Model (PRISM, Daly et al., 2008), the PPR study  
173 area receives 6% more precipitation on average than the NP study area (626 mm yr<sup>-1</sup> relative to  
174 592 mm yr<sup>-1</sup>, respectively) and 1.5% less evaporative demand or potential evapotranspiration  
175 (PET) (603 mm yr<sup>-1</sup> relative to 594 mm yr<sup>-1</sup>, respectively). These differences were not found to  
176 be statistically different using the Wilcoxon rank sum test.

177 Our regression analysis used eight-digit Hydrologic Unit Codes (HUC8s; USDA NRCS,  
178 2015) as the unit of analysis (n=150) across all eleven Landsat path/rows (Figure 1). HUC8s  
179 were used instead of smaller watersheds such as HUC10s or HUC12s to ensure that patterns in  
180 surface-water expansion and contraction represented landscape patterns, not individual or small  
181 groups of water features. HUC8s that occurred at the edge of a Landsat path/row with an area of  
182 < 50 ha were excluded from further regression analysis to limit the inclusion of incompletely  
183 characterized watersheds. The threshold of 50 ha was selected as it was a natural break in the  
184 distribution of HUC8 sizes. Patterns of surface-water expansion and contraction were compared  
185 between the PPR and NP. We note that one path/row (p37r26) in northern Montana was  
186 technically within the most western section of the PPR, but was found to behave dissimilarly  
187 from the PPR and similarly to the NP in terms of both its landscape characteristics (e.g., stream  
188 density, wetland density) and surface-water expansion and contraction. Because of this, p37r26  
189 was included in the adjacent NP for analyses where findings were organized by PPR and NP.

190

## 191 **2.2 Landsat Image Processing**

### 192 *2.2.1 Path-Row and Image Selection*





193 Surface-water extent was mapped for a series of images across 11 Landsat path/rows  
194 (Figure 1). These path/rows were selected to represent the PPR and adjacent NP and were  
195 intentionally selected to represent a range of ecoregions, climate conditions (west to east and  
196 north to south) and densities of wetlands and streams. Snow-free images (acquired  
197 approximately from April through October) containing less than 10% cloud cover from the  
198 Landsat 4-5 TM, Landsat 7 ETM+ (prior to failure of the scan-line corrector in 2003) and  
199 Landsat 8 OLI sensors were selected between 1985 and 2015. The number of images processed  
200 within each path/row averaged 14 (range: 9 to 17 acceptable images) and were intentionally  
201 selected to document interannual variability in surface-water extent, by selecting images from  
202 wet, average and dry years (Table 1). The terms “wet”, “average” and “dry” were defined in  
203 reference to local norms, using the Palmer Hydrological Drought Index (PHDI) and the 12-  
204 month Standardized Precipitation Index (SP12) (NOAA, NCDC, 2014). The range of conditions  
205 captured by the time series within each path/row in relation to the historical climate conditions  
206 (1895-2015) are shown in Table 1. The PHDI is based on a monthly water balance accounting  
207 approach that considers precipitation, evapotranspiration, runoff and soil moisture. The indices  
208 rely on weather station data and are interpolated at 5 km (NOAA NCDC, 2014). A complete list  
209 of images included in the analysis is presented in the Appendix (Table A1).

210

### 211 *2.2.2 Image Processing*

212 Images were atmospherically corrected and converted to surface reflectance values using  
213 the Landsat Ecosystem Disturbance Adaptive Processing System (Masek et al., 2006). A  
214 minimum noise fraction transformation was applied to reduce within-image noise (Green et al.,  
215 1988). The per-pixel water fraction was estimated using the Matched Filtering algorithm, a



216 partial unmixing method in the ENVI software package (Exelis Visual Information Solutions,  
217 Inc, Herndon, Va) (Turin, 1960; Vanderhoof et al., 2016). This algorithm is trained on a water  
218 spectral signature, which was derived from open-water polygons manually selected within each  
219 path/row, resulting in a water signature specific to each image. The water fraction output was  
220 linearly stretched to maximize our ability to separate water from non-water. CFmask, a quality  
221 control layer provided with Landsat images, was used to mask out clouds and cloud shadows  
222 (Zhu and Woodcock, 2014), while the National Land Cover Database (NLCD) (2011) was used  
223 to mask out impervious surfaces, defined as low, medium and high density development (Homer  
224 et al., 2015), which can show spectral confusion with surface water. Each surface-water image  
225 was visually inspected for quality using visual interpretation as well as ancillary datasets (e.g.,  
226 National Agricultural Imagery Program (NAIP) imagery, National Wetland Inventory (NWI)  
227 dataset (USFWS, 2010)). Select images were removed or edited primarily due to spectral  
228 confusion between water and bare rock or shadowed vegetation.

229

### 230 *2.2.3 Surface-Water Extent Validation*

231 The surface-water extent maps were validated using 1-m resolution NAIP imagery.  
232 Landsat images were selected for validation based on the temporal coincidence of the Landsat  
233 and NAIP imagery collections (Table 2). Because terrestrial surface water is a relatively rare  
234 cover type, it is difficult to generate enough inundated reference points through a simple random-  
235 point generation. Therefore, random points were generated in reference to NWI polygons  
236 overlapping with the NAIP and Landsat imagery. Points were then visually identified as  
237 inundated or non-inundated using the NAIP imagery. To account for the scale difference  
238 between a random point and a 900 m<sup>2</sup> Landsat pixel, the Landsat pixel boundaries for each



239 random point were identified. The point was classified as the majority class (inundated or non-  
240 inundated) identified by NAIP within the Landsat pixel boundary surrounding each random  
241 point. Reference points were generated per Landsat/NAIP pair (500 or 1000), with the number of  
242 reference points varying depending on the amount of NAIP imagery available within the Landsat  
243 path/row extent, and the number of random points that occurred within Landsat NA pixels.  
244 Metrics presented included overall accuracy, omission error, commission error, dice coefficient,  
245 and relative bias. Omission and commission errors were calculated for the category “water”. The  
246 dice coefficient is the conditional probability that if one classifier (product or reference data)  
247 identifies a pixel as water, the other one will as well, and therefore integrates omission and  
248 commission errors (Fleiss, 1981; Forbes, 1995). The relative bias provides the proportion that  
249 water is under (negative) or overestimated (positive).

250       The Landsat per-pixel fraction water was binned into inundated ( $\geq 0.3$ ) and non-  
251 inundated ( $< 0.3$ ) classes. This threshold was selected as it best balanced errors of omission and  
252 commission. Overall accuracy for the Landsat surface-water maps across the 11 path/rows was  
253 93.9% with errors of omission for surface water averaging 8.5% and errors of commission for  
254 surface water averaging 8.2% (Table 3). The surface-water maps showed no relative bias and a  
255 dice coefficient of 92%. Errors of omission and commission can be primarily attributed to mixed  
256 Landsat pixels occurring over small wetlands (a few pixels in size) or at the edge of larger  
257 wetlands or open water features. In some images parts of or entire agricultural fields were  
258 classified as water. It is common in both the spring months, when crops need to be planted, and  
259 fall months, when crops are being harvested, for fields to experience wet conditions (Fausey et  
260 al., 1987; King et al., 2014). In addition, poorly drained soil is common across this region  
261 (Skaggs et al., 1994) and wetland depressions often occur within agricultural fields.



262 Consequently, subsurface tile drainage has become increasingly popular across the region to  
263 speed up the removal of excess soil water (Blann et al., 2009). It is often unclear to what extent  
264 surface-water mapped within agricultural fields represents historical or current wetlands, poorly  
265 drained fields, or misclassified pixels. Lastly, a close match in acquisition date between the  
266 Landsat and NAIP images is essential for the NAIP imagery to accurately represent ground  
267 conditions. Variability in the date match can be considered one potential source of error, as the  
268 occurrence of a rain event or seasonal variability can change surface-water conditions over even  
269 short time periods.

270

### 271 **2.3 Surface-Water Extent Analysis**

272 Surface-water abundance ( $\text{ha km}^{-2}$ ) was calculated per HUC8 with HUC8 area being  
273 adjusted for each image based on the abundance of not applicable (NA) pixels (e.g., cloud cover,  
274 cloud shadow) in each image. We used the high-resolution National Hydrography Dataset (NHD,  
275 1:24,000) to classify surface water as (1) continuous connected with the stream network, or (2)  
276 disconnected from the stream network. The NHD line dataset was buffered by 14 m, the reported  
277 digital horizontal accuracy of the dataset (USGS, 2000) and NHD area was added to account for  
278 the width of large rivers. Surface-water polygons that intersected the stream network in a given  
279 image were classified as continuously connected water (CCW). Surface-water polygons that did  
280 not intersect the stream network in a given image were classified as discontinuous water (DCW)  
281 or discontinuous from the stream network. We acknowledge that the NHD is known to be  
282 incomplete (e.g., lacking short and ephemeral stream lines) and that some stream lines within the  
283 NHD are disconnected from downstream waters (Heine et al., 2004). However, the NHD is the  
284 most complete nationally-available stream dataset.



285           Processed images within each path/row were ranked from least-to-most amount of  
286 surface water per area. Median condition was defined as the image or two images representing  
287 the median amount of surface-water extent, estimated from all images within a path/row.  
288 Drought and deluge conditions were defined as the average of the two end-member images  
289 showing the least and most amount of total surface-water extent for each path/row, respectively.  
290 Surface-water extent was then summed across the PPR and NP path/rows and divided by the  
291 total area to calculate the hectares of surface-water extent per km<sup>2</sup> for each region. The NP  
292 portion of path 27, row 30 (p27r30) and p30r30 were deleted, as was the PPR portion of p26r30  
293 to avoid double counting overlapped path/rows.

294

#### 295 **2.4 Stage One – Derivation of the Surface Water Climate Variable (SWCR)**

296           In stage one, surface-water extent in each HUC8 was related, using linear regression, to  
297 water availability, defined as precipitation minus PET summed over a time interval. Water  
298 availability provided an estimate of the amount of water in each watershed available to either (1)  
299 runoff, (2) infiltrate to shallow or deep groundwater sources, or (3) be stored as surface-water.  
300 Surface water was again partitioned into CCW and DCW using its spatial relationship to the  
301 NHD. Precipitation data were compiled using the Parameter-elevation Regressions on  
302 Independent Slopes Model (PRISM, Daly et al., 2008). PET, or the atmospheric demand for  
303 evaporation and transpiration in the absence of water limitations, which can be expected over  
304 open surface water, was compiled using gridded surface meteorological data PRISM and the  
305 North American Land Data Assimilation System Phase 2 (Abatzoglou et al., 2011). PET was  
306 calculated using the Penman-Monteith equation that required inputs of minimum and maximum  
307 temperature, daily average dewpoint temperature (equivalently, vapor pressure or vapor pressure



308 deficit), wind speed and downward shortwave radiation (Abatzoglou et al., 2011, Mitchel et al.,  
309 2004). The datasets were resampled to 125 m using cubic convolution and summarized for each  
310 HUC8. Water availability was summed for a series of monthly periods preceding each image  
311 date (3, 6, 9, 12, 18, 24, 30 and 36 months) to identify the accumulation period for which the  
312 greatest number of HUC8's showed a significant ( $p < 0.05$ ) slope between water availability and  
313 surface-water extent. This logic was meant to reduce the probability that a zero slope resulted  
314 from surface water responding more strongly to climate drivers at a different time interval. This  
315 first stage produced surface water climate response (SWCR), our dependent variables for stage 2,  
316 i.e., the slope of the relationship between CCW and DCW surface-water extent to accumulated  
317 water availability (Figure 2). The slope or stage 2 dependent variable is referred to as the surface  
318 water climate response (SWCR) from this point forward.

319 Cloud cover makes it challenging to restrict analysis of Landsat imagery to a specific  
320 season, while including imagery that covers more than one season potentially conflates seasonal  
321 surface-water dynamics with interannual surface-water dynamics. The influence of seasonal  
322 change in surface-water extent within our analysis contributed to the uncertainty (primarily  
323 through sampling error) in the SWCR. For example, if we included an image from June 1993 and  
324 one from August 1993 and related both images to the last nine months of precipitation and PET  
325 (Sept 1992 - May 1993 and November 1992 – July 1993, respectively), greater seasonal  
326 dynamics or variation in surface-water extent between the two dates can be expected to show up  
327 as greater uncertainty in the slope, defined by the standard error of the slope or standard error of  
328 the SWCR. This becomes more evident as the accumulated period becomes larger (e.g., 36  
329 months). By explicitly considering the uncertainty of the SWCR in the regression analysis, as



330 described below in the Stage 2 Analysis (Section 2.6), we can, to the extent possible, account for  
331 seasonally induced variation in surface-water extent.

332

### 333 **2.5 Landscape Variables for Stage 2 Analysis**

334 The independent variables summarized for each HUC8 and included in the analysis were  
335 selected to characterize mechanisms through which water can leave the landscape (e.g.,  
336 infiltration, runoff, tile drainage), mechanisms through which water can remain and expand on  
337 the landscape (e.g., wetland density, wetland size, topography), as well as other potential  
338 influences on surface water dynamics (e.g., climate norms, land cover). The National Wetland  
339 Inventory (USFWS, 2010) and NHD stream dataset (USGS, 2013) were used to calculate  
340 wetland and stream characteristics including stream density, wetland count and areal density, and  
341 proportion of total wetland area attributed to large (>8 ha) features. A threshold of 8 hectares was  
342 selected as this is the size threshold used by USFWS to define a lacustrine system (Cowardin et  
343 al., 1979). We do not refer to these features as lakes, however, as water depth and associated  
344 vegetation are also important features to defining lacustrine systems, and were not evaluated. We  
345 did not include distance variables, which were previously found to be highly correlated with  
346 simpler variables already in the analyses: mean wetland-to-wetland distance was previously  
347 found to be highly correlated with wetland density ( $r = -0.95$ ,  $p < 0.01$ ) and mean wetland-to-  
348 stream distance highly correlated with stream density ( $r = 0.88$ ,  $p < 0.01$ ) (Vanderhoof et al.,  
349 2017). Surface topography can influence the capacity for surface water to expand and was  
350 quantified as the weighted averaged slope gradient, as defined by the U.S. Department of  
351 Agriculture's Soil Survey Geographic (SSURGO) Database (Soil Survey Staff, 2017).  
352 Topographic Wetness Index was not included because of the relative weakness of such indices in



353 landscapes with little relief (e.g., Schmidt and Persson, 2003) and the data intensive nature of  
354 calculating TWI with a 10 m DEM across such a large study area. Additional variables derived  
355 from the SSURGO database to characterize infiltration capacity include available water storage  
356 (0 - 150 cm), annual minimum depth to water table, and saturated hydraulic conductivity (Ksat).  
357 Human influence was quantified as the abundance of agricultural activities, or the percent of  
358 each HUC8 classified as agriculture, defined as the NLCD (2011) cover categories hay/pasture  
359 and row crop. Anthropogenic modifications to drainage systems, or the percent land cover  
360 artificially drained, was estimated as the percent of each HUC8 where row crop cover type  
361 (NLCD 2011) and very poorly drained or poorly drained soils as defined by the National  
362 Resources Conservation Service's SSURGO database were collocated following Christensen et  
363 al., (2013). The climate normals per HUC8 (1989-2013) were calculated to represent the Landsat  
364 image range. The precipitation averages are provided as part of the PRISM dataset (Daly et al.,  
365 2008). PET was calculated as a function of monthly mean PRISM temperature and day length  
366 following Hamon (1961). The Moisture Index (MI) was calculated as the ratio of precipitation  
367 and PET where, if PET exceeded precipitation,  $MI = \text{precipitation}/PET - 1$ , and if precipitation  
368 exceed or equaled PET, then  $MI = 1 - PET/\text{precipitation}$ . Values range from -1 (dry) to 1 (wet)  
369 (Willmott and Feddema, 1992; Feddema, 2005). The climate averages were resampled to 1 km  
370 from 4 km using inverse-distance weighting, prior to being averaged per HUC8. The distribution  
371 of values within each of the independent variables are shown in Table 4. Spearman rank  
372 correlations with a Bonferroni correction (Dunn, 1961) were calculated for the independent  
373 variables (Table 5).

374

## 375 **2.6 Stage 2 - Analysis - Landscape Mechanisms Explaining Variability in SWCR**





376 In stage two, CCW and DCW SWCRs, or the slope of the relationship between CCW and  
377 DCW and accumulated water availability, were related to landscape variables using feasible  
378 generalized least-squares (FGLS) regression, with HUC8s (n=150) as the unit of analysis. FGLS  
379 allowed us to estimate the heteroscedastic structure of the residuals (Lewis and Linzer, 2005) and  
380 has been previously applied within landscape ecology contexts (e.g., Acharya, 2000; Villalobos-  
381 Jimenéz and Hassall, 2017). The SWCRs were found to be significant for the largest number of  
382 HUC8s using a 9-month period of accumulation for both CCW and DCW, which was therefore  
383 used as the accumulation period for further analyses (Table 6). The SWCRs were found to be  
384 spatially autocorrelated using Global Moran's I (spatial relationship conceptualized using inverse  
385 distance) (DCW SWCR, 9 months, z-score=7.8,  $p<0.01$ , CCW SWCR, 9 month, z-score=4.1,  
386  $p<0.01$ ), violating the assumption of independence between samples. To account for spatial  
387 autocorrelation in the SWCRs, we calculated an autocovariate in ArcGIS 10.3, Geostatistical  
388 Analyst (ESRI, Redmond CA) which uses adjacent HUC8s to create a neighbor value. By  
389 including a spatial autocovariate in the ordinary least-squares (OLS) regression model, we  
390 controlled for how much the response variable reflected response values of adjacent HUCs,  
391 before identifying additional significant explanatory variables (Dormann et al., 2007; Betts et al.,  
392 2009). The autocovariate was automatically retained while only significant independent variables  
393 ( $p<0.05$ ) were additionally retained. The dependent variable was normalized using a Box-Cox  
394 power transformation (R package MASS, Venables and Ripley, 2002). Multicollinearity was  
395 formally assessed using the regression collinearity diagnostics described by Belsley et al. (1980)  
396 and implemented in the R package perturb (Hendrickx, 2012). Collinearity may affect parameter  
397 estimation when a condition index greater than 10 is associated with variance decomposition



398 proportions greater than 0.5 for two or more explanatory variables (Belsley, 1991). Both models  
399 complied with collinearity requirements.

400 Having an estimated dependent variable (e.g., SWCR) does not necessarily present a  
401 problem for a regression analysis, but we must recognize that the regression model error term  
402 contains two components: (1) the expected random error resulting from sources of variation not  
403 accounted for in the model, and (2) the difference between the true value of the dependent  
404 variable and the estimated value (sampling error). In this study, the uncertainty around the  
405 dependent variable (SWCR) was not constant across observations. Instead, the dependent  
406 variable showed a strong positive correlation with its standard error (DCW SWCR,  $R^2 = 0.59$ ,  
407  $p < 0.05$ ; CCW SWCR,  $R^2 = 0.70$ ,  $p < 0.05$ ) (Figure 3). FGLS allowed us to estimate both  
408 components of the error. To do so, we: (1) calculated the logarithm of squared residuals from the  
409 OLS model, (2) regressed the log-residuals on the independent variables included in the OLS  
410 model, (3) calculated the exponential of fitted values from that regression, which estimates the  
411 variance of the regression residual that is not due to sampling of the dependent variable,  $z$ , and  
412 (4) estimated the basic model again now including weights ( $1/z^2$ ) (Hanushek, 1974; Lewis and  
413 Linzer, 2005). We found the final model residuals to be random using the studentized Breusch-  
414 Pagan test (Breusch and Pagan, 1979).

415 To help add confidence regarding which landscape variables were more or less important,  
416 we also fit random forest models in R using the package randomForest (Liaw and Wiener, 2015).  
417 The random forests were run with the SWCRs as the dependent variable and landscape  
418 characteristics as independent variables. We derived 500 binary trees or bootstrap iterations  
419 using out of bag (OOB) samples (70% of samples to train and 30% of samples to validate).  
420 Variable importance was calculated as the change in node impurity (i.e., Gini importance).



421 Random forest models are generally insensitive to collinearity among metrics, however the  
422 inclusion of correlated variables can deflate variable importance as well as the overall variation  
423 explained by the model (Murphy et al., 2010). We implemented random forest model selection to  
424 select the smallest number of non-redundant variables (varSelRF R package) (Murphy et al.,  
425 2010).

426

### 427 **3 Results**

#### 428 **3.1 Surface-Water Extent**

429 Median surface-water extent as well as the amount of water added and lost from the  
430 surface between wet and dry periods was found to vary considerably across the study area  
431 (Figure 4 and 5). Analysis of the median total surface-water extent between the PPR and the NP  
432 demonstrated that the PPR had 2.6 times greater surface-water extent than the NP (Table 7). The  
433 PPR also showed greater variability in total surface-water extent, adding 5.7 ha km<sup>-2</sup> during very  
434 wet conditions and losing 2.8 ha km<sup>-2</sup> during very dry conditions, for a maximum net difference  
435 of 8 ha km<sup>-2</sup>. This can be compared to the NP which gained 1.6 ha km<sup>-2</sup> during very wet  
436 conditions and lost 0.8 ha km<sup>-2</sup> during very dry conditions, a net difference of 2.4 ha km<sup>-2</sup> (Table  
437 7). DCW, or water that was discontinuous with the stream network, showed greater expansion  
438 and contraction in extent in both the PPR and NP, relative to CCW which intersected the stream  
439 network. Consequently, DCW increased as a percent of total surface water during wet periods  
440 and decreased as a percent of total surface water in dry periods. This suggests that across the  
441 study area, surface water that was disconnected from the stream network disproportionately  
442 served a surface water storage function during wet periods, reducing the amount of water



443 contributing to downstream flooding. Similarly, DCWs disproportionately experienced loss  
444 during dry periods.

445

### 446 **3.2 Relationship between Surface-Water Extent and Water Availability**

447 Including PET instead of using precipitation alone tended to increase the percentage of  
448 HUC8s showing a statistically significant relationship between surface-water extent and water  
449 availability across the different accumulation periods that we tested, although this was not true  
450 for all time periods. For instance, the percent change from precipitation to precipitation minus  
451 PET ranged from -1.4 to 38% for DCW and -6.3 to 24.3% for CCW. For DCW there was a jump  
452 in the percentage of HUC8s showing a significant relationship between six and nine months, but  
453 the percentage of HUC8s stabilized after this time period out to 36 months. CCW showed a  
454 similar but smaller jump in the percentage of HUC8s with a significant relationship between six  
455 and nine months (Table 6). At nine months, all images, regardless of being collected in the  
456 spring, summer or fall, would include winter precipitation. We observed substantial spatial  
457 variability in the statistical relationship between surface-water extent and water availability.  
458 Using nine months as the accumulation period, we observed a strong spatial pattern in DCW.  
459 PPR HUC8s tended to show a greater SWCR, exhibited by a substantial increase in surface-  
460 water extent with increased water availability, while HUC8s across the NP tended to show a  
461 smaller SWCR, exhibited by minor to no increases in surface-water extent with increased water  
462 availability (Figure 6 and 7). For CCW, the spatial pattern was less consistent within the PPR or  
463 ecoregion boundaries. Instead, HUC8s with a greater SWCR tended to be HUC8s with large  
464 lakes or floodplains (Figure 6 and 7).

465



### 466 3.3 Landscape Variables Explaining Variability in Surface-Water Response

467 For DCW SWCR, when independent variables were assessed individually using  
468 Spearman's rank correlation, the SWCR was greater in locations with fewer streams ( $R = -0.64$ ,  
469  $p < 0.05$ ), lower slope gradient ( $R = -0.59$ ,  $p < 0.05$ ), higher wetland density ( $R = 0.52$ ,  $p < 0.05$ ) and  
470 total wetland area ( $R = 0.51$ ,  $p < 0.05$ ), deeper minimum depth to water table ( $R = 0.59$ ,  $p < 0.05$ )  
471 and where a greater proportion of the total surface water was disconnected from the stream  
472 network ( $R = 0.42$ ,  $p < 0.05$ ) (Table 8). When the relative importance of the variables was tested  
473 using random forest, variables found to be the most important included, wetland density, stream  
474 density, annual minimum depth to water table and the slope gradient (Table 8). However, after  
475 accounting for the spatial autocorrelation in the DCW SWCR and the significance of the  
476 variables, the DCW SWCR increased in the final feasible generalized least-squares model  
477 (adjusted  $R^2 = 0.66$ , F-statistic = 73.6) with (1) greater wetland density, (2) deeper depth to  
478 groundwater, and (3) less anthropogenic drainage (Table 9). The variable most consistent  
479 identified across statistical approaches was wetland density.

480 For CCW SWCR, fewer independent variables showed a significant Spearman rank  
481 correlation. The SWCR for stream-connected water increased in locations with a greater total  
482 wetland area ( $R = 0.48$ ,  $p < 0.05$ ) and less average precipitation ( $R = -0.33$ ,  $p < 0.05$ ) (Table 8).  
483 Using random forest, the total wetland area and proportion of total water from large features  
484 were found to be the most important variables in explaining variation. The final feasible  
485 generalized least-squares model (adjusted  $R^2 = 0.54$ , F-statistic = 37.4) also found the  
486 relationship between CCW and surface-water availability (i.e., SWCR) was stronger with greater  
487 total wetland area, but also found that it decreased with greater wetland density (Table 9).

488



489 **4. Discussion**

490 Surface-water extent, and in particular surface water within well-studied portions of the  
491 PPR, has been previously shown to exhibit seasonal and interannual patterns (Poff et al., 1997;  
492 Beeri and Phillips, 2007; Vanderhoof et al., 2016) that can, in turn, influence the cumulative  
493 hydrologic response of a watershed (Golden et al. 2016; Evenson et al. 2016; Ali and Creed  
494 2017). What has been less studied is how surface-water dynamics vary across diverse  
495 landscapes. This is particularly relevant when we consider the need for communities and local  
496 agencies to plan ahead for expected changes in the precipitation regime associated with climate  
497 change (Dore, 2005; Johnson et al., 2005; Millett et al., 2009). Our results demonstrated that the  
498 relationship between surface-water extent and water availability (SWCR) is a function of both  
499 climate and landscape variables and that the density of depressional wetlands, in particular,  
500 played a key explanatory role in the observed landscape response to increased climate inputs.  
501 Given our findings, we expect that changes in net precipitation from climate change or other  
502 climatic forcings will disproportionately affect surface-water extent across the PPR relative to  
503 the adjacent NP, and that these effects will be more evident in disconnected wetland systems  
504 (DCWs) than in wetlands connected to the river network (CCWs). Surface waters that are  
505 disconnected from the stream network showed a larger change in extent in response to wetter  
506 conditions in landscapes with higher wetland densities. That is to say that landscapes with a  
507 larger number of depressional features were found to show a greater increase in surface-water  
508 extent in response to a wetter climate, relative to landscapes with fewer depressional features. In  
509 landscapes with more concentrated water, greater total wetland area, but lower wetland density,  
510 surface waters connected to the stream network showed more substantial expansion with  
511 increased water availability. This finding suggests that the presence of stream-connected lakes



512 within large flat basins may be an important factor influencing surface-water expansion.  
513 Previous research found lakes within the PPR to be important features that commonly experience  
514 extensive surface-water expansion, subsuming adjacent wetlands during wet periods  
515 (Vanderhoof and Alexander, 2016). These findings suggest that if climate conditions within the  
516 U.S. portion of the PPR continue to get wetter, as predicted (e.g., Millett et al. 2009), then both  
517 small wetland depressions and larger features, such as lakes and floodplains, will both serve  
518 critical roles in storing increased inputs of surface water, which could prevent downstream  
519 flooding.

520 Our study area was intentionally selected to encompass a large area with a wide range of  
521 landscape conditions in regards to wetland and stream density and capacity for infiltration.  
522 Across the study area, variation in the values of many of the variables (e.g., stream density,  
523 wetland density) can be attributed to landscape age or the time since the last glacial retreat, and  
524 corresponding variability in drainage development across the region (Ahnert, 1996). The  
525 Wisconsin glacier retreated from the PPR by 11,300 BP, meaning the drainage system is still  
526 developing and surface water is being stored in glacially formed depressions (Winter and  
527 Rosenberry, 1998; Stokes et al., 2007). In contrast, the landscape to the west and south of the  
528 PPR, is much older (>20,000 BP) with a well-developed drainage network (Clayton and Moran,  
529 1982).

530 In addition to extensive human-induced wetland loss across the region (Miller et al.,  
531 2009; Van Meter et al., 2015), the drainage network across the region is also increasingly  
532 modified with the expansion of ditch networks and tile drainage in association with agricultural  
533 activities (McCauley et al., 2015). Ditches, pipes and field tiles on the glacial till can hasten the  
534 speed with which water leaves a location and lower the water table through increased water



535 withdrawal (De Laney, 1995; Blann et al., 2009; McCauley et al., 2015). We found in the FGLS  
536 model, the expansion of disconnected water was inversely related to the abundance of estimated  
537 anthropogenic drainage. Because anthropogenic drainage increases the rate at which water leaves  
538 a location, it results in the loss or reduction of landscape-scale functions of wetlands and other  
539 natural water storage features in the PPR (McCauley et al. 2015), and shifts the hydrologic  
540 behaviors of watersheds towards those more commonly seen in the NP.

541 Evapotranspiration is known to be a primary mechanism for water loss in the PPR  
542 (Winter and Rosenberry, 1998). By explicitly incorporating this value into the SWCR, we could  
543 better isolate the effects of landscape-based components such as surface storage, stream density,  
544 and topography. One challenging component to characterize was the capacity for water to  
545 infiltrate through soil horizons. Depth to bedrock SSURGO data was found to be too patchy (i.e.,  
546 too much missing data) to be useful. A variable that instead was found to correlate significantly  
547 with the expansion of disconnected water was annual minimum depth to groundwater. The PPR  
548 tended to have a deeper minimum depth while the NP had a shallower minimum depth, on  
549 average. A reduction in infiltration due to the low permeability of glacial till (Sloan, 1972;  
550 Winter and Rosenberry, 1995), would reduce the potential for increased water table elevations.  
551 Concomitantly, with less infiltration, pulses of snowmelt or precipitation in the PPR would  
552 instead be transported as overland flow and fill wetlands with available storage.

553 We must also consider that we may be missing key landscape variables that could explain  
554 variability in the spatial response of surface-water extent to climate inputs. For example, major  
555 landscape characteristics required for stream-connected surface water to expand include (1)  
556 large, stream-connected water bodies such as lakes and (2) hydrologically-connected floodplains.  
557 The influence of large water bodies was considered by including total wetland area and the





558 portion of water from larger (>8 ha) features, however we did not explicitly consider the  
559 presence/absence of active floodplains beyond including stream density as a variable. Floodplain  
560 activity typically exhibits strong seasonal patterns; however, the goal of our analysis was to  
561 focus on patterns of surface-water extent that occurred on longer-time scales (i.e., interannual  
562 variability). Because of this, we excluded two Landsat path/rows from the analysis that were  
563 originally included because strong seasonal flooding outweighed interannual patterns in climate  
564 as evidenced by a lack of a relationship between climate indices (e.g., Standardized Precipitation  
565 Index (12 months) and Palmer Hydrologic Drought Index) and surface-water extent. These  
566 path/rows included p30r27 which straddles North Dakota and Minnesota and exhibits strong  
567 seasonal flooding of the Red River and p28r32 in the southeastern corner of Nebraska, which  
568 exhibits strong seasonal flooding of the Missouri River. However, even with the exclusion of  
569 these two path/rows, the importance of floodplains is still evident in Figure 6B where we  
570 observed greater SWCR in areas with an abundance of lakes or floodplain systems. Because  
571 complete floodplain maps across the study area are lacking, we were not able to explicitly  
572 identify the role of floodplains in the CCW models.

573 In addition to decision points regarding study area extent, other decision points may have  
574 influenced our findings. For example, the period of time for which the greatest number of  
575 HUC8s showed a significant SWCR was used as the climate accumulation period. This logic was  
576 meant to avoid, to the extent possible, a HUC8 showing a zero SWCR because surface water  
577 responded at a time period different than the one selected. However, its usage meant that the  
578 study results are limited to interpreting the relationship of surface-water extent to same year  
579 climate inputs (or the previous 9 months) and may be less applicable to understanding the  
580 relationship of surface-water extent to shorter (seasonal) or longer (multi-year) time periods. In



581 addition, decisions regarding image inclusion may have also influenced the analysis. Although  
582 the Landsat images used in the analysis were selected strategically to represent historically dry,  
583 average, and wet conditions, because the Landsat images were processed individually we were  
584 ultimately limited in the number of Landsat images we could process. As more remotely sensed  
585 products become available, such as the U.S. Geological Survey's Dynamic Surface Water Extent  
586 (DSWE) Product, which plans to utilize the entire Landsat archive (1984 to present) (Jones,  
587 2015), we could utilize many more images and reduce the uncertainty in estimates of the SWCR  
588 or watershed-specific response to available water. Although decision points regarding the data  
589 included or excluded from the analysis are important to consider, this study provides an  
590 improved understanding of how the relationship between surface-water extent and climate may  
591 vary spatially across different landscapes.

592

## 593 **5. Conclusion**

594 Shifts in climate patterns and the frequency of extreme climate events will influence  
595 surface-water extent. This has implications for habitat availability (Boschilia et al., 2008;  
596 Calhoun et al., 2017), agricultural productivity (Mokrech et al., 2008; Gornall et al., 2010) and  
597 hydrologic connectivity (Golden et al. 2016; Ali and Creed 2017). This study demonstrated that  
598 not only is surface-water extent variable across landscapes, but shifts in climate patterns will  
599 have an uneven effect on surface-water extent across these different landscapes. The PPR  
600 experienced a 2.6 fold greater surface-water extent than the adjacent NP under average  
601 conditions and a 3.4 fold larger range in surface-water extent between drought and deluge  
602 conditions. To move from ecoregion boundaries to a more functional characterization of the  
603 spatial distribution of surface water on the landscape, we used a statistical approach to explore



604 potentially significant landscape variables that could explain the spatially variable change in  
605 surface water to climate inputs (precipitation minus evapotranspiration). Landscapes with higher  
606 wetland density and less anthropogenic drainage showed a greater expansion of disconnected  
607 (from the stream network) surface water (e.g., depressional wetlands) and wetter climatic  
608 conditions relative to landscapes with fewer wetlands and more anthropogenic drainage.  
609 Landscapes with fewer wetlands but more total surface water area (e.g., lakes, large river  
610 systems) showed a greater expansion of stream-connected surface water and wetter climatic  
611 conditions relative to landscapes with less total surface water area. Enhancing our knowledge of  
612 spatial and temporal variability in the relationship between surface-water extent and climate  
613 inputs can advance efforts to predict the hydrologic effects of climate change, including drought  
614 and floods, on water resources and improve hydrological modeling in low gradient landscapes.  
615

## 616 **Acknowledgements**

617 This research was funded by the Drought Resilience Initiative through an interagency agreement  
618 with the U.S. Environmental Protection Agency, Office of Research and Development (DW-014-  
619 92454401 - 0). We thank Tedros Berhane, Hayley Distler, Marena Gilbert and Clifton Burt for  
620 their assistance in processing the Landsat imagery and ancillary datasets. We thank Maliha Nash  
621 for providing data on climate averages. The views expressed in this manuscript are solely those  
622 of the authors and do not necessarily reflect the views or policies of the U.S. EPA. Any use of  
623 trade, firm, or product names is for descriptive purposes only and does not imply endorsement by  
624 the U.S. Government.

625

## 626 **6. References**



- 627 Abatzoglou, J. T.: Development of gridded surface meteorological data for ecological  
628 applications and modelling, *Int. J. Climatol.*, 33, 121-131, 2011.
- 629 Acharya, G.: Approaches to valuing the hidden hydrological services of wetland ecosystems,  
630 *Ecol. Econ.*, 35, 63-74, 2000.
- 631 Ahnert, F.: Introduction to Geomorphology, John Wiley & Sons, New York, 1996.
- 632 Allen, C. R., Angeler, D. G., Cumming, G. S., Carl, F., and Twidwell, D.: Quantifying spatial  
633 resilience, *J. Appl. Ecol.*, 53, 625-635, 2016.
- 634 Ameli, A. A., Creed, I. F.: Quantifying hydrologic connectivity of wetlands to surface water  
635 systems, *Hyrol. Earth Syst. Sci.*, 21, 1791-1808, 2017.
- 636 Beeri, O. and Phillips, R. L.: Tracking palustrine water seasonal and annual variability in  
637 agricultural wetland landscapes using Landsat from 1997 to 2005, *Glob. Change Biol.*, 13,  
638 897-912, 2007.
- 639 Belsley, D. A.: Conditioning Diagnostics, Collinearity and Weak Data in Regression, John Wiley  
640 & Sons, New York, 1991.
- 641 Belsley, D. A., Kuh, E., and Welsch, R.E.: Regression Diagnostics: Identifying Influential Data  
642 and Sources of Collinearity, John Wiley & Sons, New York, 1980.
- 643 Betts, M. G., Ganio, L. M., Huso, M. M. P., Som, N. A., Huettmann, F., Bowman, J., and Wintle,  
644 B. A.: Comment on “Methods to account for spatial autocorrelation in the analysis of species  
645 distributional data: A review.”, *Ecography*, 32, 374-378, 2009.
- 646 Blann, K. L., Anderson, J. L., Sands, G. R., and Vondracek, B.: Effects of agricultural drainage  
647 on aquatic ecosystems: A review, *Crit. Rev. Environ. Sci. Technol.*, 39, 909-1001,  
648 doi:10.1080/10643380801977966, 2009.
- 649 Boschilia, S. M., Oliveira, E. F., and Thomaz, S. M.: Do aquatic macrophytes co-occur  
650 randomly? An analysis of null models in a tropical floodplain, *Oecologia*, 156, 203-214,  
651 2008.
- 652 Breusch, T. S. and Pagan, A. R.: A simple test for heteroskedasticity and random coefficient  
653 variation, *Econometrica*, 47, 1287-1294, JSTOR 1911963, MR 545960, 1979.
- 654 Bryson, R. A. and Hare, F. K.: Climates of North America, in: *World Survey of Climatology*,  
655 Vol. 11, Lansberg, H. E., (Ed.), Elsevier, New York, 47 pp., 1974.
- 656 Calhoun, A. J. K., Mushet, D. M., Bell, K. P., Boix, D., Fitsimons, J. A., and Isselin-Nondedeu,  
657 F.: Temporary wetlands: challenges and solutions to conserving a “disappearing” ecosystem,  
658 *Biol. Conserv.*, 211, 3-11, 2017.
- 659 Carroll, R. W., Pohll, G. M., Tracy, J., Winter, T., and Smith, R.: Simulation of a semipermanent  
660 wetland basin in the Cottonwood Lake Area, East-Central North Dakota, *J. Hydrol. Eng.*, 1,  
661 70-84, 2005.
- 662 Christensen, J. R., Nash, M. S., and Neale, A.: Identifying riparian buffer effects on stream  
663 nitrogen in southeastern coastal plain watersheds, *Environ. Manage.* 52, 1161-1176, 2013.
- 664 Clayton, L. and Moran, S. R.: Chronology of late Wisconsinan glaciation in middle North  
665 America, *Quaternary Sci. Rev.*, 1, 55-82, 1982.
- 666 Cohen, M. J., Creed, I. F., Alexander, L., Basu, N., Calhoun, A., Craft, C. B., D’Amico, E.,  
667 DeKeyser, S., Fowler, L., Golden, H., Jawitz, J. W., Kalla, P., Kirkman, L. K., Lane, C. R.,  
668 Lang, M., Leibowitz, S., Lewis, D. B., Marton, J. M., McLaughlin, D. L., Mushet, D.,  
669 Raanan-Kipperwas, H., Rains, M. C., Smith, L., and Walls, S.: Do geographically isolated  
670 wetlands influence landscape functions?, *P. Natl. Acad. Sci. U.S.A.*, 113, 1978-1986, doi:  
671 10.1073/pnas.1512650113, 2016.



- 672 Cowardin, L. M., Carter, V., Golet, F. C., and LaRoe, E. T.: Classification of wetlands and  
673 deepwater habitats of the United States, U.S. Fish and Wildlife Service, Washington, DC,  
674 FWS/OBS-79/31, 1979.
- 675 Daly, C., Halbleib, M., Smith, J. I., Gibson, W. P., Doggett, M. K., Taylor, G. H., Curtis, J., and  
676 Pasteris, P. A.: Physiographically-sensitive mapping of temperature and precipitation across  
677 the conterminous United States, *Int. J. Climatol.*, 28, 2031-2064, doi: 10.1002/joc.1688,  
678 2008.
- 679 De Laney, T. A.: Benefits to downstream flood attenuation and water quality as a result of  
680 constructed wetlands in agricultural landscapes, *J. Soil Water Conserv.*, 50, 620-626, 1995.
- 681 Dore, M. H. I.: Climate change and changes in global precipitation patterns: What do we know?,  
682 *Environ. Int.*, 31, 1167-1181, 2005.
- 683 Dormann, C. F., McPherson, J. M., Araujo, M. B., Bivand, R., Bolliger, J., Carl, G., Davies, R.  
684 G., Hirzel, A., Jetz, W., Kissling, W. D., Kühn, I., Ohlemüller, R., Peres-Neto, P. R.,  
685 Reineking, B., Schröder, B., Schurr, F. M., and Wilson, R.: Methods to account for spatial  
686 autocorrelation in the analysis of species distributional data: A review, *Ecography*, 30, 609–  
687 628, 2007.
- 688 Dunn, O. J.: Multiple comparison among means, *J. Am. Stat. Assoc.*, 56, 52–64, 1961.
- 689 Eamus, D., Hatton, T., Cook, P., and Colvin, C.: *Ecohydrology: vegetation function, water and  
690 resource management*, CSIRO Publishing, Australia, 360 pp., 2006.
- 691 Euliss Jr., N. H. and Mushet, D. M.: Water-level fluctuation in wetlands as a function of  
692 landscape condition in the Prairie Pothole Region, *Wetlands*, 16, 587–59, 1996.
- 693 Evenson, G. R., Golden, H. E., Lane, C. R., D’Amico, E.: An improved representation of  
694 geographically isolated wetlands in a watershed-scale hydrologic model, *Hydrol Processes*,  
695 doi:10.1002/hyp.10930, 2016.
- 696
- 697 Fausey, N. R., Doering, E. J., and Palmer, M. L.: Purposes and benefits of drainage, in: *Farm  
698 drainage in the United States: History, status, and prospects*, Pavelis, G. A. (Ed.), USDA  
699 Economic Research Service, Washington, DC, Misc. Publ. 1455, 4 pp., 1987.
- 700 Feddema, J. J.: A revised Thornthwaite-type global climate classification, *Phys. Geogr.*, 26, 442-  
701 466, 2005.
- 702 Fleiss, J. L.: *Statistical methods for rates and proportions* (2<sup>nd</sup> ed.), John Wiley & Sons, New  
703 York City, NY, 1981.
- 704 Flint, R. F.: *Glacial and Quaternary Geology*, John Wiley & Sons, New York City, NY, 1971.
- 705 Forbes, A. D.: Classification-algorithm evaluation: Five performance measures based on  
706 confusion matrices. *J. Clinical Monitoring*, 11(3), 189-206, 1995.
- 707 Gleason, R. A. and Tangen, B. A.: Ecosystem services derived from wetland conservation  
708 practices in the United States prairie pothole region with an emphasis on the U.S., in:  
709 Department of Agriculture Conservation Reserve and Wetlands Reserve Programs  
710 Professional Paper 1745: Floodwater storage, Gleason, R. A., Laubhan, M. K., Euliss Jr., M.  
711 K. (Eds.), U.S. Geological Survey, Reston, VA, 7 pp., 2008.
- 712 Golden, H. E., Sander, H. A., Lane, C. R., Zhao, C., Price, K., D’Amico, E., Christensen, J.R.:  
713 Relative effects of geographically isolated wetlands on streamflow: A watershed-scale  
714 analysis, *Ecohydrology*, 9(1), 21-38, 2016.
- 715 Golden, H. E., Creed, I. F., Ali, G., Basu, N. B., Neff, B. P., Rains, M. C., McLaughlin, D. L.,  
716 Alexander, L. C., Ameli, A. A., Christensen, J. R., Evenson, G. R., Jones, C. N., Lane, C. R.,



- 717 and Lang, M.: Integrating geographically isolated wetlands into land management decisions,  
718 *Front. Ecol. Environ.*, 15, 319-327, 2017.
- 719 Gornall, J., Betts, R., Burke, E., Clark, R., Camp, J., Willett, K., and Wiltshire, A.: Implications  
720 of climate change for agricultural productivity in the early twenty-first century, *Philos. Trans.*  
721 *R. Soc. B. Biol. Sci.*, 365, 2973–2989, 2010.
- 722 Green, A. A., Berman, M., Switzer, P., and Craig, M. D.: A transformation for ordering  
723 multispectral data in terms of image quality with implications for noise removal, *IEEE T.*  
724 *Geosci. Remote*, 26, 65–74, 1988.
- 725 Hamilton, S. K., Sippel, S. J., and Melack, J. M.: Comparison of inundation patterns among  
726 major South American floodplains, *J. Geophys. Res.*, 107, 1-14, 2002.
- 727 Hamilton, S. K., Sippel, S. J., and Melack, J. M.: Seasonal inundation patterns in two large  
728 savanna floodplains of South America: the Llanos de Moxos (Bolivia) and the Llanos del  
729 Orinoco (Venezuela and Colombia), *Hydrol. Process*, 18, 2103–2116, 2004.
- 730 Hamon, W. R.: Estimating potential evapotranspiration, *J. Hydr. Eng. Div. ASCE*, 87, 107-120,  
731 1961.
- 732 Hanushek, E. A.: Efficient estimators for regressing regression coefficients, *Am. Stat.*, 28, 66–  
733 67, 1974.
- 734 Heiler, G., Hein, T., Schiemer, F., and Bornette, G.: Hydrological connectivity and flood pulses  
735 as the central aspects for the integrity of a river-floodplain system, *Regul. River*, 11, 351–  
736 361, 1995.
- 737 Heine, R. A., Lant, C. L., Sengupta, R. R.: Development and comparison of approaches for  
738 automated mapping of stream channel networks. *Annals of the Assoc of Am Geographers*,  
739 94(3), 477–490, 2004.
- 740 Hendrickx, J.: Perturb: Tools for evaluating collinearity, R package version 2.05,  
741 <http://CRAN.R-project.org/package=perturb>, 2012.
- 742 Hoffmann, C. C., Kjaergaard, C., Uusi-Kämpä, J., Hansen, H. C., and Kronvang, B.:  
743 Phosphorus retention in riparian buffers: Review of their efficiency, *J. Environ. Qual.*, 38,  
744 1942-1955, 2009.
- 745 Homer, C., Dewitx, J., Yang, L., Jin, S., Danielson, P., Xian, G., Coulston, J., Herold, N.,  
746 Wickham, J., and Megown, K.: Completion of the 2011 National Land Cover Database for  
747 the conterminous United States – representing a decade of land cover change information,  
748 *Photogramm. Eng. Rem. S.*, 81, 345–354, 2015.
- 749 Huang, S., Dahal, D., Young, C., Chander, G., and Liu, S.: Integration of Palmer Drought  
750 Severity Index and remote sensing data to simulate wetland water surface from 1910 to 2009  
751 in Cottonwood Lake area, North Dakota, *Remote Sens. Environ.*, 115, 3377-3389, 2011.
- 752 Johnson, W. C., Millett, B. V., Gilmanov, T., Voldseth, R. A., Guntenspergen, G. R., and  
753 Naugle, D. E.: Vulnerability of northern prairie wetlands to climate change, *Bioscience*, 55,  
754 863–872, 2005.
- 755 Jones, J. W.: Efficient wetland surface water detection and monitoring via Landsat: comparison  
756 with in situ data from the Everglades depth estimation network, *Remote Sens.*, 7, 12503-  
757 12538, 2015.
- 758 Kahara, S. N., Mockler, R. M., Higgins, K. F., Chipps, S. R., and Johnson, R. R.: Spatiotemporal  
759 patterns of wetland occurrence in the Prairie Pothole Region of eastern South Dakota,  
760 *Wetlands*, 29, 678-689, 2009.





- 761 Kantrud, H. A., Krapu, G. L., and Swanson, G. A.: Prairie basin wetlands of the Dakotas: a  
762 community profile, U.S. Fish and Wildlife Service Biological Report 85(7.28), Washington,  
763 DC, 1989.
- 764 King, K. W., Fausey, N. R., and Williams, M. R.: Effect of subsurface drainage on streamflow in  
765 an agricultural headwater watershed, *J. Hydrol.*, 519, 438–445, 2014.
- 766 Kuppel, S., Houspanossian, J., Noretto, M. D., and Jobbágy, E. G.: What does it take to flood the  
767 Pampas? Lessons from a decade of strong hydrological fluctuations, *Water Resour. Res.*, 51,  
768 2937–2950, doi:10.1002/2015WR016966, 2015.
- 769 LaBaugh, J. W., Winter, T. C., and Rosenberry, D. O.: Hydrologic functions of prairie wetlands,  
770 *Great Plains Res.*, 4, 17–37, 1998.
- 771 Lewis, J. B. and Linzer, D. A.: Estimating regression models in which the dependent variable is  
772 based on estimates, *Polit. Anal.*, 13, 345–364, 2005.
- 773 Liaw, A. and Wiener, M.: Breiman and Cutler’s random forests for classification and regression,  
774 R package version 4.6-12, R Foundation for Statistical Computing, Vienna, Austria,  
775 <https://www.stat.berkeley.edu/~breiman/RandomForests/>, 2005.
- 776 Masek, J. G., Vermote, E. F., Saleous, N., Wolfe, R., Hall, E. F., Huemmrich, F., Gao, F., Kutler,  
777 J., and Teng-Kui, L.: A Landsat surface reflectance data set for North America, 1990–2000,  
778 *IEEE Geosci. Remote S.*, 3, 68–72, 2006.
- 779 McCauley, L. A., Anteau, M. J., Van Der Burg, M. P., and Wiltermuth, M. T.: Land use and  
780 wetland drainage affect water levels and dynamics of remaining wetlands, *Ecosphere*, 6, 1–  
781 20, 2015.
- 782 Millett, B., Johnson, W. C., and Guntenspergen, G.: Climate trends of the North American  
783 Prairie Pothole Region 1906–2000, *Climatic Change*, 93, 243–267, 2009.
- 784 Mitchell, K. E., Lohmann, D., Houser, P. R., Wood, E. F., Schaake, J. C., Robock, A., Cosgrove,  
785 B. A., Sheffield, J., Duan, Q., Luo, L., Higgins, R. W., Pinker, R. T., Tarpley, J. D.,  
786 Lettenmaier, D. P., Marshall, C. H., Entin, J. K., Pan, M., Shi, W., Koren, V., Meng, J.,  
787 Ramsay, B. H., and Bailey, A. A.: The multi-institution North American Land Data  
788 Assimilation System (NLDAS): Utilizing multiple GCIP products and partners in a  
789 continental distributed hydrological modeling system, *J. Geophys. Res.*, 109, D07S90,  
790 doi:10.1029/2003JD003823, 2004.
- 791 Mokrech, M., Nicholls, R. J., Richards, J. A., Henriques, C., Holman, I. P., and Shackley, S.:  
792 Regional impact assessment of flooding under future climate and socio-economic scenarios  
793 for East Anglia and North West England, *Climatic Change*, 90, 31–55, 2008.
- 794 Murphy, M. A., Evans, J. S., and Storfer, A.: Quantifying *Bufo boreas* connectivity in Yellowstone  
795 National Park with landscape genetics, *Ecology*, 91, 252–261, 2010.
- 796 Niemuth, N. D., Wangler, B., and Reynolds, R. E.: Spatial and temporal variation in wet area of  
797 wetlands in the prairie pothole region of North Dakota and South Dakota, *Wetlands*, 30,  
798 1053–1064, 2010.
- 799 NOAA National Climatic Data Center: Data Tools: 1981–2010 Normals,  
800 <http://www.ncdc.noaa.gov/cdo-web/datatools/normals>, last access: 12, January, 2017, 2014.
- 801 Poff, N. L., Allan, J. D., Bain, M. B., Karr, J. R., Prestegard, K. L., Richter, B. D., Sparks, R.  
802 E., and Stromberg, J. C.: The natural flow regime, *BioScience*, 47, 769–784, 1997.
- 803 Pringle, C. M.: Hydrologic connectivity and the management of biological reserves: a global  
804 perspective, *Ecol. Appl.*, 11, 981–998, 2001.



- 805 Rosenberry, D. O., Stannard, D. I., Winter, T. C., and Martinez, M. L.: Comparison of 13  
806 equations for determining evapotranspiration from a prairie wetland, Cottonwood Lake area,  
807 North Dakota, USA, *Wetlands*, 24, 483–497, 2004.
- 808 Sass, G. Z. and Creed, I. F.: Characterizing hydrodynamics on boreal landscapes using archived  
809 synthetic aperture radar imagery, *Hydrol. Process.*, 22, 1687–1699, 2008.
- 810 Sayler, K. L., Acevedo, W., Soulard, C. E., and Taylor, J. L.: Land cover trends dataset, 2000–  
811 2011, U.S. Geological Survey, <http://dx.doi.org/10.5066/F7DJ5CNT>, 2015.
- 812 Schmidt, F., Persson, A.: Comparison of DEM data capture and topographic wetness indices,  
813 *Precision Agriculture*, 4(2), 179–192, 2003.
- 814 Shaw, D. A., Vanderkamp, G., Conly, F. M., Pietroniro, A., and Martz, L.: The fill-spill  
815 hydrology of prairie wetland complexes during drought and deluge, *Hydrol. Process.*, 26,  
816 3147–3156, 2012.
- 817 Skaggs, R. W., Breve, M. A., and Gilliam, J. W.: Hydrologic and water quality impacts of  
818 agricultural drainage, *Crit. Rev. Environ. Sci. Technol.*, 24, 1–32,  
819 doi:10.1080/10643389409388459, 1994.
- 820 Sloan, C. E.: Ground-water hydrology of Prairie Potholes in North Dakota, U.S. Geological  
821 Survey Professional Paper, 585, 1–27, 1972.
- 822 Smith, L. C., Sheng, Y., and MacDonald, G. M.: A first pan-arctic assessment of the influence of  
823 glaciation, permafrost, topography and peatlands on northern hemisphere lake distribution,  
824 *Permafrost Periglac.*, 18, 201–208, 2007.
- 825 Stokes, C. R., Popovnin, V., Aleynikov, A., Gurney, S. D., and Shahgedanova, M.: Recent  
826 glacier retreat in the Caucasus Mountains, Russia, and associated increase in supraglacial  
827 debris cover and supra-/proglacial lake development, *Ann. Glaciol.*, 46, 195–203, 2007.
- 828 Turin, G.: An introduction to matched filters, *IRE T. Inform. Theor.*, 6, 311–329, 1960.
- 829 U.S. Department of Agriculture, National Resources Conservation Service: Watershed Boundary  
830 Dataset,  
831 <http://www.nrcs.usda.gov/wps/portal/nrcs/detail/national/water/watersheds/dataset/?cid=nrcs>  
832 143\_021625, last access: 20 September 2016, 2015.
- 833 U.S. Department of Agriculture, Natural Resources Conservation Service: Soil Survey  
834 Geographic (SSURGO) Database, <https://sdmdataaccess.sc.egov.usda.gov>, last access: 25  
835 May 2017, 2017.
- 836 U.S. Fish and Wildlife Service: National Wetlands Inventory, <http://www.fws.gov/wetlands/>, last  
837 access: 1 September 2016, 2010.
- 838 U.S. Geological Survey: The National Hydrography Dataset (NHD) concepts and content,  
839 available at: [http://nhd.usgs.gov/chapter1/chp1\\_data\\_users\\_guide.pdf](http://nhd.usgs.gov/chapter1/chp1_data_users_guide.pdf), 2010.
- 840 U.S. Geological Survey: The National Hydrography Dataset (NHD),  
841 [ftp://nhdftp.usgs.gov/DataSets/Staged/States/FileGDB/ HighResolution](ftp://nhdftp.usgs.gov/DataSets/Staged/States/FileGDB/HighResolution), last access: 2  
842 September 2017, 2013.
- 843 van der Kamp, G. W., Stolte, J., and Clark, R. G.: Drying out of small prairie wetlands after  
844 conversion of their catchments from cultivation to permanent brome grass, *Hydrolog. Sci. J.*,  
845 44, 387–397, 1999.
- 846 Van Meter, K. J. and Basu, N. B.: Signatures of human impact: size distributions and spatial  
847 organization of wetlands in the Prairie Pothole landscape, *Ecol. Appl.*, 25, 451–465, 2015.
- 848 Vanderhoof, M. K., Alexander, L. C., and Todd, M. J.: Temporal and spatial patterns of wetland  
849 extent influence variability of surface water connectivity in the Prairie Pothole Region,  
850 United States, *Landscape Ecol.*, 31, 805–824, 2016.





- 851 Vanderhoof, M. K. and Alexander, L. C.: The role of lake expansion in altering the wetland  
852 landscape of the Prairie Pothole Region, *Wetlands*, 36, 309-321, 2016.
- 853 Vanderhoof, M. K., Christensen, J. R., and Alexander, L. C.: Patterns and drivers for wetland  
854 connections in the Prairie Pothole Region, United States, *Wetl. Ecol. Manag.*, 25, 275-297,  
855 2017.
- 856 Venables, W. N. and Ripley, B. D.: *Modern Applied Statistics with S*, Fourth Edition, Springer,  
857 New York, 2002.
- 858 Villalobos-Jimenez, G. and Hassall, C.: Effects of the urban heat island on the phenology of  
859 Odonata in London, UK, *Int. J. Biometeorol.*, 61, 1337-1346, 2017.
- 860 Wagener, T., Sivapalan, M., Troch, P., and Woods, R.: Catchment classification and hydrologic  
861 similarity, *Geogr. Compass*, 1, 901-931, 2007.
- 862 Wiche, G. G.: Lake levels, streamflow, and surface-water quality in the Devil's Lake Area, North  
863 Dakota, U.S. Geological Survey Fact Sheet, Bismarck, ND, 8 pp., 1996.
- 864 Willmott, C. J. and Feddema, J. J.: A more rational climatic moisture index, *Prof. Geogr.*, 44, 84-  
865 88, 1992.
- 866 Winter, T. C.: The concept of hydrologic landscapes, *J. Am. Water Res. Assoc.*, 37, 335-349,  
867 2001.
- 868 Winter, T. C. and Rosenberry, D. O.: The interaction of ground water with Prairie Pothole  
869 wetlands in the Cottonwood Lake area, east-central North Dakota, 1979–1990, *Wetlands*, 15,  
870 193–211, 1995.
- 871 Winter, T. C. and Rosenberry, D. O.: Hydrology of prairie pothole wetlands during drought and  
872 deluge: 7-year study of the Cottonwood Lake wetland complex in North Dakota in the  
873 perspective of longer term measured and proxy hydrological records, *Climatic Change*, 40,  
874 189-209, 1998.
- 875 Yao, T., Pu, J., Lu, A., Wang, Y., and Yu, W.: Recent glacial retreat and its impact on  
876 hydrological processes on the Tibetan Plateau, China, and surrounding regions, *Arct. Antarct.  
877 Alp. Res.*, 39, 642-650, 2007.
- 878 Zhang, B., Schwartz, F. W., and Liu, G.: Systematics in the size structure of prairie pothole lakes  
879 through drought and deluge, *Water Resour. Res.*, 45, W04421, 2009.
- 880 Zhu, Z. and Woodcock, C. E.: Automated cloud, cloud shadow, and snow detection in  
881 multitemporal Landsat data: An algorithm designed specifically for monitoring land cover  
882 change, *Remote Sens. Environ.*, 152, 217-234, 2014.
- 883
- 884
- 885
- 886



887 **Tables**

888 **Table 1.** A summary of the Landsat images utilized within each selected path/row. Landsat TM images were used for dates 2011 and  
 889 earlier. Landsat 8 OLI images were used for 2013 forward. DOY: day of year; PHDI: Palmer Hydrological Drought Index. \*p37r26  
 890 was considered NP because of its dissimilarity with the rest of the PPR.

Path/Row	PPR/Northern Prairie (NP (primary)	Number of Images	Spring (DOY 60-151)	Summer (DOY 152-243)	Fall (DOY 244-335)	Year Range	Min. PHDI (%)	Max. PHDI (%)	Mean PHDI (%)
p26r30	NP	12	6	4	2	1987-2010	4	99	45
p26r32	NP	17	10	3	4	1988-2010	2	99	51
p27r30	PPR	9	3	4	2	1988-2008	4	99	54
p29r29	PPR	17	9	2	6	1990-2011	7	100	69
p30r30	PPR	13	5	5	3	1988-2013	2	100	45
p30r31	NP	15	6	5	4	1986-2011	5	94	38
p31r27	PPR	15	2	6	7	1990-2011	3	100	67
p31r29	PPR	13	6	5	2	1989-2011	7	99	45
p33r28	NP	15	8	2	5	1988-2015	1	99	49
p36r28	NP	16	7	7	2	1985-2013	2	96	38
p37r26	NP*	15	4	6	5	1987-2013	1	99	52
<b>Total</b>		<b>157</b>	<b>66</b>	<b>49</b>	<b>42</b>				

891



892 **Table 2.** Landsat images and corresponding National Agricultural Imaging Program (NAIP) images used to validate the Landsat  
 893 surface-water extent maps. Accuracy is presented here by Landsat image. PHDI: Palmer Hydrological Drought Index, SPI2: 12 month  
 894 Standardized Precipitation Index, OE: omission error for water, CE: commission error for water, OA: overall accuracy, DC: Dice  
 895 coefficient, RB: relative bias

Landsat Path/Row	Landsat date	NAIP date(s)	Gap (days)	PHDI	SPI2	Number of points	OE (%)	CE (%)	OA (%)	DC (%)	RB (%)
p26r32	28-Jun-04	23-Jun-04 and 07-Jul-04	-5 to +9 days	0.57	0.14	947	6.3	5.9	97.4	93.9	-0.5
p27r30	14-Jul-13	10-Jul-13 and 12-Jul-13	-4 to -2 days	-0.34	0.05	707	11.8	9.3	92.5	89.5	-2.7
p29r29	13-Oct-06	25-Sep-06	-18 days	2.3	-0.08	814	11.1	2.5	93.6	93.0	-8.8
p29r29	8-Oct-10	17-Sep-10 and 20-Sep-10	+18 to +21 days	9.63	3.06	959	1.9	3.3	97.4	96.4	1.4
p31r29	17-Jul-04	10-Jul-04 and 14-Jul-04	-7 to -3 days	-0.4	-0.04	1302	7.4	1.5	97.2	95.4	-6.0
p33r28	13-Jul-03	11-Jul-03 and 15-Jul-03	-2 to +2 days	-2.74	-0.91	908	10.6	27.0	85.5	80.4	22.5
p37r26	31-Jul-11	16-Jul-11 and 19-Jul-11	-15 to -12 days	2.96	1.29	498	16.8	9.7	90.2	86.6	-7.9

896

897 **Table 3.** Summary of accuracy statistics across all of the Landsat images validated using National Agricultural Imaging Program  
 898 (NAIP) imagery.

	NAIP - Inundated	NAIP - Non-Inundated	Total
Landsat - Inundated	2052	183	2235
Landsat - Non-Inundated	190	3710	3900
Total	2242	3893	6135
Omission error for water (%)	8.5		
Commission error for water (%)	8.2		
Overall Accuracy (%)	93.9		
Dice Coefficient	91.7		
Relative Bias	0.0		

899

900



901 **Table 4.** Independent variables considered in the landscape analysis and the distribution of values for each variable across the 8-digit  
 902 hydrological units (HUC8s). Mean values for the HUC8s within the Prairie Pothole Region (PPR) and Northern Prairie (NP) are also  
 903 shown with significant differences ( $p < 0.01$ ) between the two groups, as determined by the Wilcoxon rank sum test, indicated by  
 904 different superscript letters. NHD: National Hydrography Dataset, NWI: National Wetland Inventory, PRISM: Parameter-elevation  
 905 Regressions on Independent Slopes Model, SSURGO: Soil Survey Geographic Database, NLCD: National Land Cover Database,  
 906 DCW: disconnected surface water, PET: potential evapotranspiration, avg: average

Independent Variables	Units	Range	25th %	50th %	75th %	PPR (avg)	NP (avg)	Source
<b>Wetland and Stream Characteristics</b>								
Stream density	m ha <sup>-1</sup>	0.1 to 26.1	7.2	11.4	15.0	7.8 <sup>a</sup>	14.5 <sup>b</sup>	High-Resolution NHD (USGS 2013)
Total wetland density	no ha <sup>-1</sup>	0 to 0.2	0.02	0.03	0.06	0.06 <sup>a</sup>	0.03 <sup>b</sup>	NWI (USFWS 2010)
Total wetland areal abundance	ha ha <sup>-1</sup>	0 to 0.7	0.02	0.03	0.08	0.08 <sup>a</sup>	0.05 <sup>b</sup>	NWI (USFWS 2010)
Portion of total water area from large features	%	0.1 to 97.8	32.1	44.7	58.0	45.0 <sup>a</sup>	47.2 <sup>a</sup>	NWI (USFWS 2010, Zhang et al., 2009)
Portion DCW of total surface water	%	0 to 100	10.6	24.4	50.0	44.5 <sup>a</sup>	22.8 <sup>b</sup>	Landsat and NHD (USGS 2013)
<b>Climate Averages</b>								
Moisture Index Average	~	-0.4 to 0.7	-0.1	-0.04	0.2	0.04 <sup>a</sup>	-0.03 <sup>a</sup>	PRISM (Daly et al., 2008)
Precipitation Average	mm yr <sup>-1</sup>	312.3 to 1007.8	490.3	599.6	790.8	641.5 <sup>a</sup>	624.3 <sup>a</sup>	PRISM (Daly et al., 2008)
PET Average	mm yr <sup>-1</sup>	496.2 to 683.0	564.2	595.5	628.9	595.5 <sup>a</sup>	594.8 <sup>a</sup>	PRISM (Daly et al., 2008)
<b>Soil and Topography</b>								
Available water storage (0-150 cm), weighted	cm	7.6 to 29.5	18.0	22.8	24.7	24.0 <sup>a</sup>	19.1 <sup>b</sup>	SSURGO (Soil Survey Staff, 2017)
Annual minimum depth to water table	cm	0.1 to 69.0	11	24.8	43.3	40.5 <sup>a</sup>	17.9 <sup>b</sup>	SSURGO (Soil Survey Staff, 2017)
Ksat	µm sec <sup>-1</sup>	2.1 to 107.7	8.4	13.8	22.5	21.4 <sup>a</sup>	21.2 <sup>a</sup>	SSURGO (Soil Survey Staff, 2017)
Slope gradient, weighted average	%	1.5 to 19.2	3.0	4.3	7.1	3.3 <sup>a</sup>	7.1 <sup>b</sup>	SSURGO (Soil Survey Staff, 2017)
<b>Human Influence</b>								
Agricultural land cover	%	0.1 to 92.0	25.2	62.8	80.5	72.6 <sup>a</sup>	39.6 <sup>b</sup>	2011 NLCD (Homer et al., 2015)
Percent drained by anthropogenic means	%	0 to 93.0	5.9	50.1	77.8	61.7 <sup>a</sup>	32.5 <sup>b</sup>	2011 NLCD and SSURGO

907

908

909



910 **Table 5.** Spearman rank correlation values between the independent variables considered in the analysis. Bonferonni correction was  
 911 applied to the p-values and significant correlations ( $p < 0.05$ ) are starred. DCW: surface water disconnected from the stream network,  
 912 CCW: continuously connected surface water, MI: Moisture Index, PET: potential evapotranspiration, precip: precipitation, lg: large,  
 913 ag: agricultural, Ksat: saturated hydraulic conductivity, na: not applicable

Variable	DCW auto-covariate	CCW auto-covariate	Portion dis- connected	Stream density	Wetland density	Wetland areal abund.	Dominance of lg. water bodies	MI	Precip	PET	Avail water storage (0- 150 cm)	Annual min depth to water table	Ksat	Slope gradient	Ag land cover	Percent drained
DCW autocovariate	1	na	0.45*	-0.66*	0.48*	0.48*	-0.04	0.03	-0.05	0.03	0.29	0.54*	0.21	-0.58*	0.33*	0.22
CCW autocovariate		1	-0.11	-0.16	0.15	0.27	0.18	-0.29	-0.26	0.15	0.05	-0.04	0.01	-0.16	-0.03	-0.07
Portion DCW of total water			1	-0.38*	0.32*	-0.09	-0.63*	0.33*	0.20	0.05	0.37*	0.54*	0.11	-0.34*	0.46*	0.26
Stream density				1	-0.33*	-0.37*	-0.05	-0.34*	-0.21	0.09	-0.34*	-0.62*	0.47*	0.66*	-0.33*	-0.2
Wetland density					1	0.79*	-0.02	0.24	0.19	-0.1	0.26	0.29	-0.03	-0.19	0.11	0.25
Wetland areal abundance						1	0.44	0.18	0.06	-0.1	0.21	0.26	-0.01	-0.29	0.05	0.23
Dominance of lg water bodies							1	-0.22	-0.16	0	-0.11	-0.1	0.08	0.1	-0.24	-0.01
MI								1	0.86*	-0.2	0.60*	0.67*	0.14	-0.41*	0.80*	0.64*
Precipitation									1	0.25	0.48*	0.44*	0.03	-0.17	0.66*	0.50*
PET										1	-0.07	-0.21	-0.2	0.12	-0.08	-0.16
Avail water storage (0-150 cm)											1	0.49*	-0.05	-0.44*	0.66*	0.51*
Annual min depth to water table												1	0.19	-0.61*	0.69*	0.57*
Ksat													1	-0.25	0.02	-0.07
Slope gradient														1	-0.63*	-0.32*
Agricultural land cover															1	0.63*



915 **Table 6.** The percent of HUC8s across the study area that showed a significant relationship ( $p < 0.05$ ) between surface-water extent and  
 916 (1) precipitation (Precip or P) or (2) precipitation minus potential evapotranspiration (PET) for different accumulation periods. DCW:  
 917 disconnected surface water; CCW: continuously, connected surface water.

Accumulated Period	Precip DCW (%)	P - PET DCW (%)	Inclusion of PET change (DCW)	Precip CCW (%)	P - PET CCW (%)	Inclusion of PET change (CCW)
3 months	19.4	27.1	7.6	15.3	28.5	13.2
6 months	5.6	31.9	<b>26.4</b>	9.0	33.3	<b>24.3</b>
9 months	20.8	<b>59.7</b>	<b>38.9</b>	27.1	<b>48.6</b>	<b>21.5</b>
12 months	45.8	50.7	4.9	42.4	41.0	-1.4
18 months	24.3	<b>58.3</b>	<b>34.0</b>	25.7	39.6	13.9
24 months	<b>52.1</b>	50.7	-1.4	<b>43.8</b>	37.5	-6.3
30 months	28.5	55.6	<b>27.1</b>	27.1	43.1	16.0
36 months	<b>54.9</b>	54.9	0.0	<b>47.2</b>	<b>44.4</b>	-2.8
HUC8s with a sig relationship in at least 1 time period	65.3	75.7	10.4	59.0	67.4	8.3



919 **Table 7.** Surface-water extent conditions summarized for the Prairie Pothole Region (PPR) and adjacent Northern Prairie (NP). TSW:  
 920 total surface-water extent, CCW: continuously connected surface water that intersects the stream network, DCW: disconnected surface  
 921 water or surface water that does not directly intersect the stream network.

Region	Path/ rows (all or part)	Total area (km <sup>2</sup> )	Min (ha km <sup>2</sup> )	Max (ha km <sup>2</sup> )	Median (ha km <sup>2</sup> )	Added min to max (ha km <sup>2</sup> )	Reduction from median to min (%)	Increase from median to max (%)	Min (%) of all (area)	Max (%) of all (area)	Median (% of all) (area)
PPR TSW	7	146,309	3.51	11.99	6.33	8.48	44.6	89.2	~	~	~
NP TSW	9	173,026	1.62	4.07	2.45	2.45	33.9	66.1	~	~	~
PPR CCW	7	146,309	2.82	7.56	4.44	4.74	36.5	70.4	80.3	63.1	70.1
NP CCW	9	173,026	1.44	3.11	2.06	1.66	30.0	50.5	89.1	76.3	84.2
PPR DCW	7	146,309	0.69	4.42	1.90	3.73	63.4	133.4	19.7	36.9	29.9
NP DCW	9	173,026	0.18	0.97	0.39	0.79	54.4	149.2	10.9	23.7	15.8

922

923



924 **Table 8.** Spearman rank correlation values between the dependent variables and each of the independent variables considered in the  
 925 analysis. Bonferroni correction was applied to the p-values and significant correlations ( $p < 0.05$ ) are starred. Relative variable  
 926 importance as determined by random forest models are also presented for each variable (i.e., increase in node purity). PET: potential  
 927 evapotranspiration, Ksat: saturated hydraulic conductivity, DCW: disconnected surface water, CCW: continuously, connected surface  
 928 water

Variable	Response (DCW, 9 months)		Response (CCW, 9 months)	
	Spearman rank correlation	Increase in node purity	Spearman rank correlation	Increase in node purity
Autocovariate	0.79*	0.081	0.53*	0.108
Portion DCW is of total surface water	0.42*	0.012	-0.11	0.334 <sup>1</sup>
Stream density	-0.64*	0.036 <sup>1</sup>	-0.15	0.060
Wetland density	0.52*	0.048 <sup>1</sup>	0.27	0.057 <sup>1</sup>
Wetland areal abundance	0.51*	0.017 <sup>1</sup>	0.48*	0.855 <sup>1</sup>
Portion of total water from large features	-0.01	0.004	0.30	0.556 <sup>1</sup>
Moisture Index (average)	-0.03	0.005	-0.28	0.053 <sup>1</sup>
Precipitation (average)	-0.10	0.008 <sup>1</sup>	-0.33*	0.039 <sup>1</sup>
PET (average)	-0.06	0.011 <sup>1</sup>	-0.13	0.034
Available water storage (0-150 cm)	0.27	0.007	-0.01	0.061
Annual minimum depth to water table	0.56*	0.027 <sup>1</sup>	0.09	0.046
Ksat	0.04	0.004	-0.08	0.070 <sup>1</sup>
Slope gradient, weighted average	-0.59*	0.025 <sup>1</sup>	-0.22	0.072
Agricultural land cover	0.31	0.005	-0.05	0.035
Percent drained by anthropogenic means	0.22	0.004	-0.04	0.020

929 <sup>1</sup>Variables selected by the random forest model selection process, using the R package rUtilities, when the autocovariate was not included.

930

931

932





933 **Table 9.** Feasible generalized least square models with residual weights applied relating the response (of surface-water extent to water  
 934 availability) to landscape-related variables. All variables included in the models were significant. DCW: surface water disconnected  
 935 from the stream network, CCW: continuously connected surface water, SE: standard error, D.F.: degrees of freedom

Response of DCW water to water availability		Variables	Coefficients	SE	t-value
D.F. = 145		Intercept	0.17	0.01	12.84
F-statistic = 73.6		Autocovariate	0.03	0.004	6.32
adjusted R <sup>2</sup> = 0.66		Wetland density	0.90	0.23	3.96
		Minimum depth to groundwater	0.0021	0.0006	3.29
		Percent anthropogenically drained	-0.0004	0.0003	-1.25
Response of CCW water to water availability		Variables	Coefficients	SE	t-value
D.F. = 144		Intercept	0.018	0.01	1.43
F-statistic = 69.4		Wetland areal abundance	0.96	0.07	14.42
adjusted R <sup>2</sup> = 0.58		Wetland density	-0.43	0.21	-2.09
		Autocovariate	-0.12	0.01	-0.89

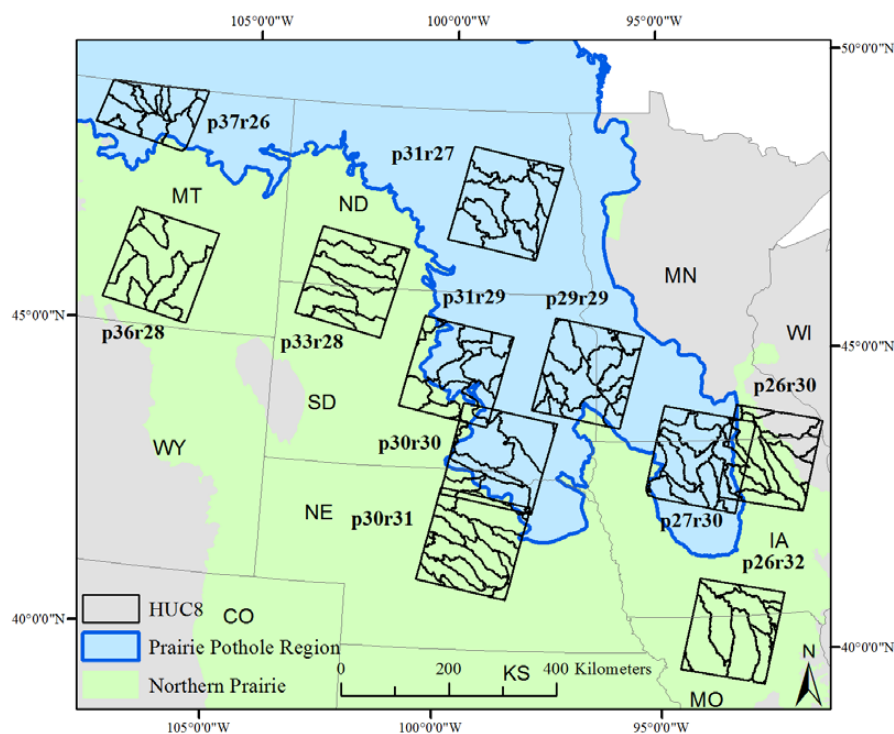
936

937

938



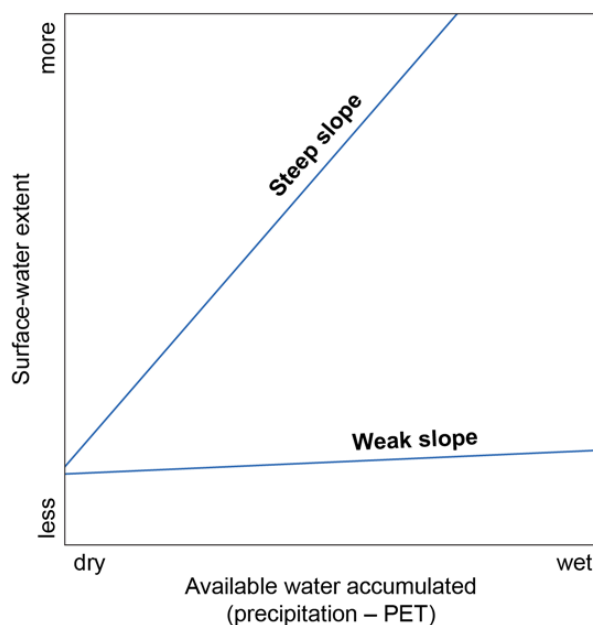
939 **Figures**



940

941 **Figure 1.** Distribution of Landsat path/rows used to map surface-water extent and corresponding  
942 8-digit Hydrological Units (HUC8s) used for further analysis in relation to the boundary of the  
943 Prairie Pothole Region (PPR). The p37r26 behaved dissimilarly from the PPR and similarly to  
944 the adjacent Northern Prairie (NP) in all regards and was therefore included with the NP for  
945 analyses organized by PPR and NP.

946



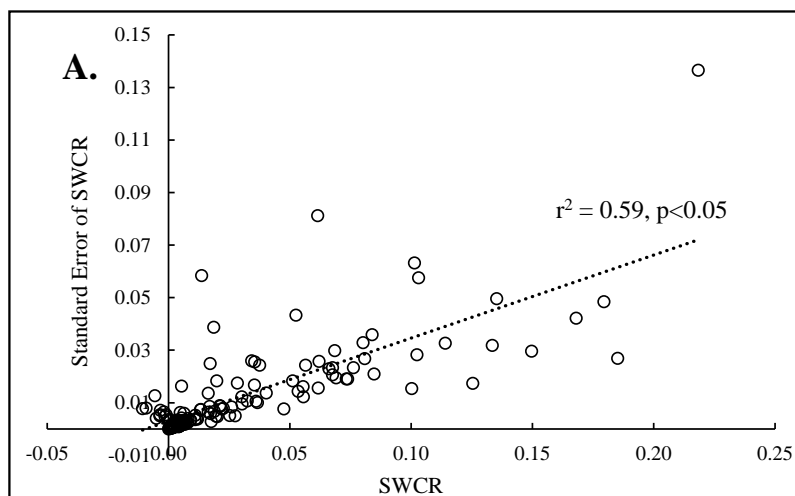
947

948 **Figure 2.** Theoretical figure showing the derived dependent variable, or the Surface Water  
949 Climate Response (SWCR), defined as the slope of the statistical relationship between  
950 accumulated water and surface-water extent. Some areas show a greater SWCR or substantial  
951 increase in surface-water extent as more water becomes available via precipitation minus  
952 potential evapotranspiration (PET), while other areas show little to no change in surface-water  
953 extent, presumably as excess water leaves the system through runoff or infiltration.

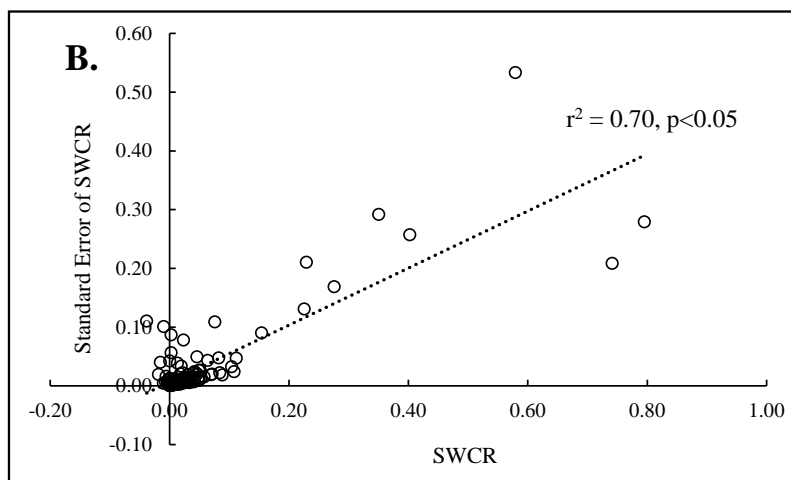
954



955

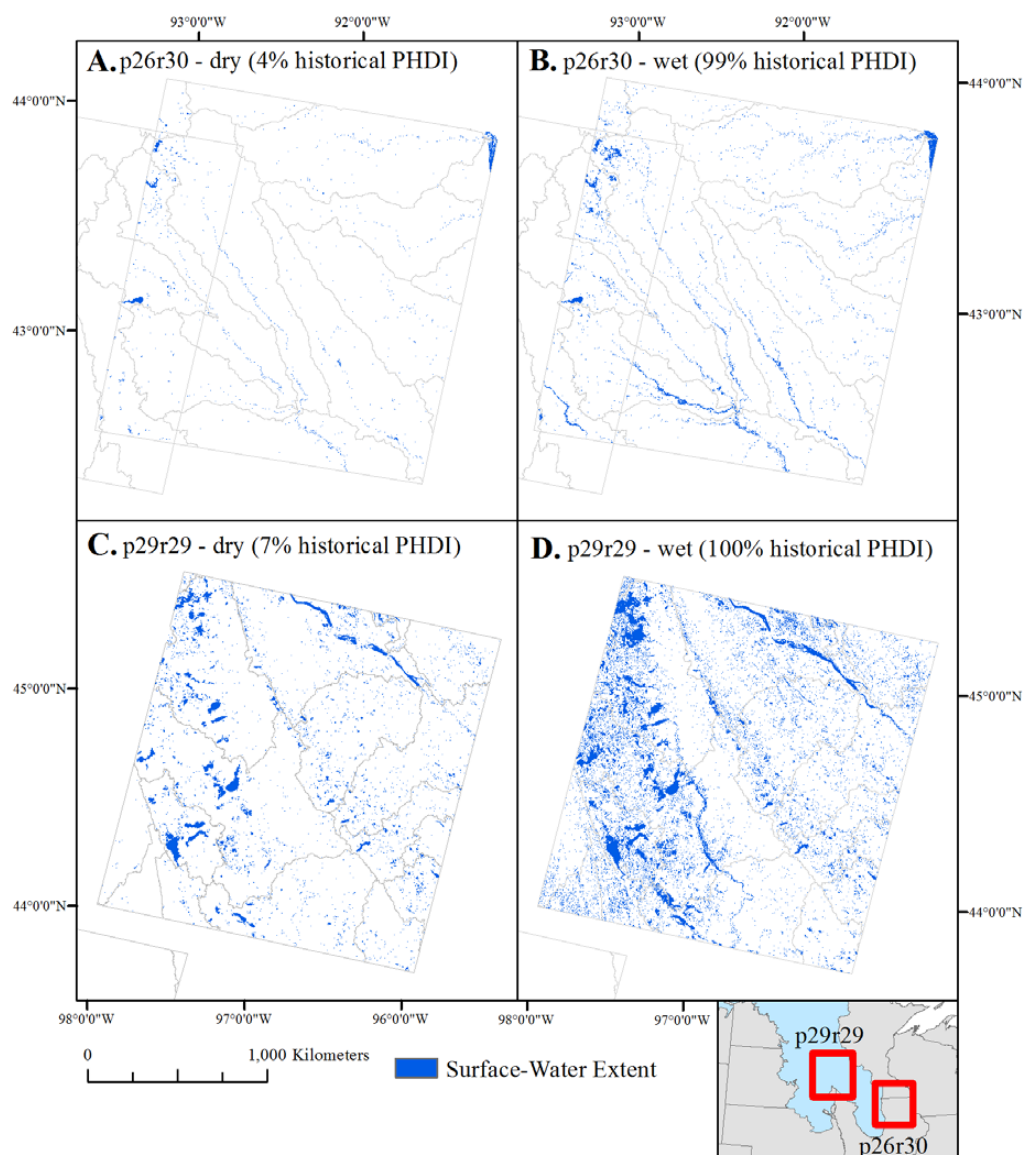


956



957 **Figure 3.** Standard errors of the Surface Water Climate Response (SWCR) tended to be  
958 positively correlated with both A) discontinuous surface water (DCW) or surface water  
959 disconnected from the stream network and B) continuously connected water (CCW) or surface  
960 water connected to the stream network.

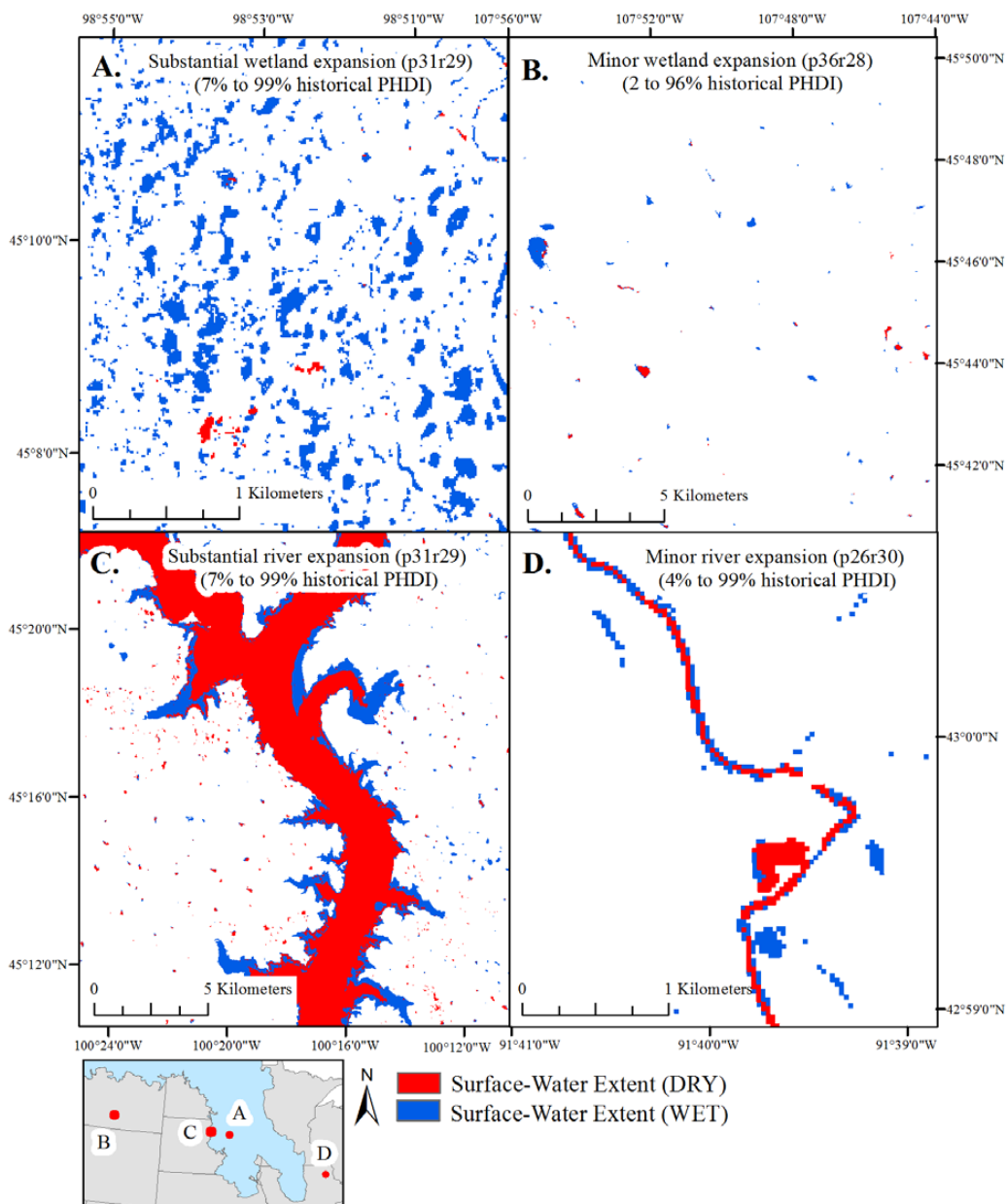
961



962

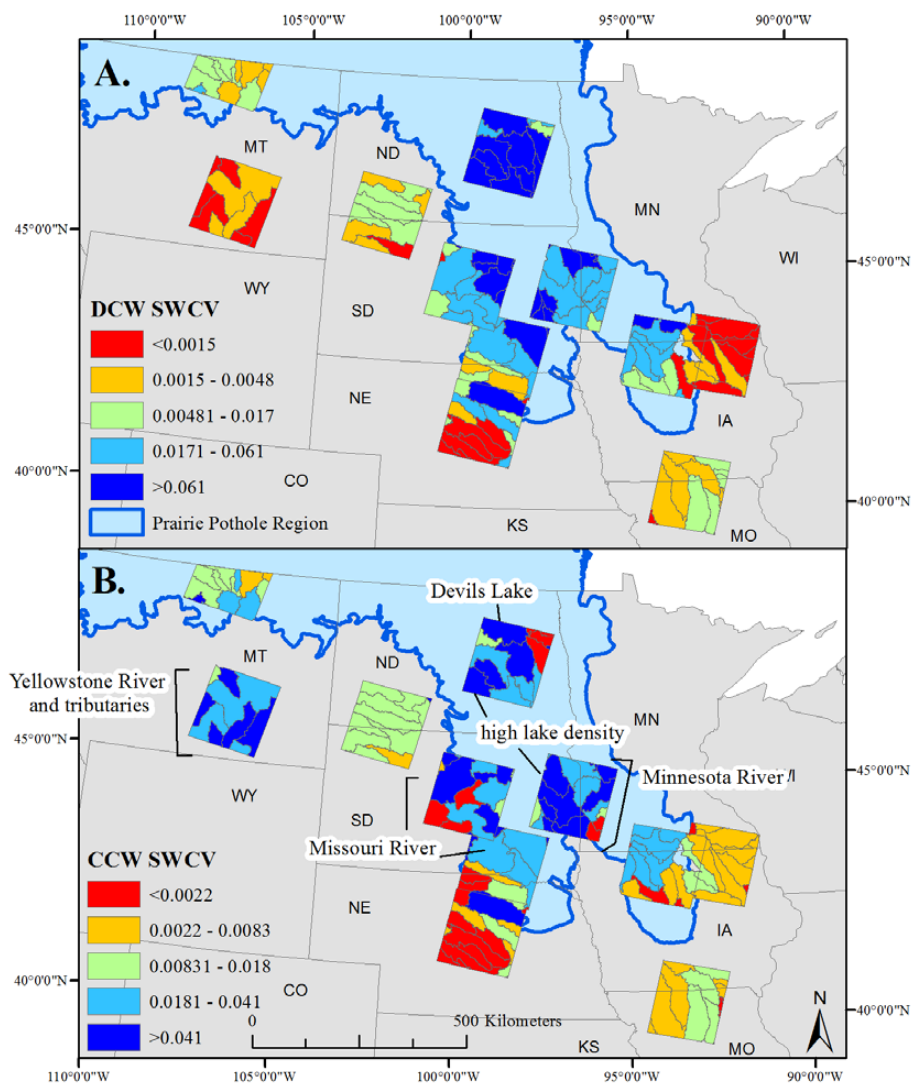
963 **Figure 4.** Mean surface-water abundance and the amount of “wetting up” varied substantially  
964 between different Landsat path/rows. Portions of the Northern Prairie (e.g., p26r30) showed  
965 relatively less surface-water extent and expansion (A and B) while portions of the Prairie Pothole  
966 Region (e.g., p29r29) showed relatively more surface-water extent and expansion (C and D).  
967 Note: not all water is visible at this zoomed-out scale. PHDI: Palmer Hydrological Drought  
968 Index

969



970

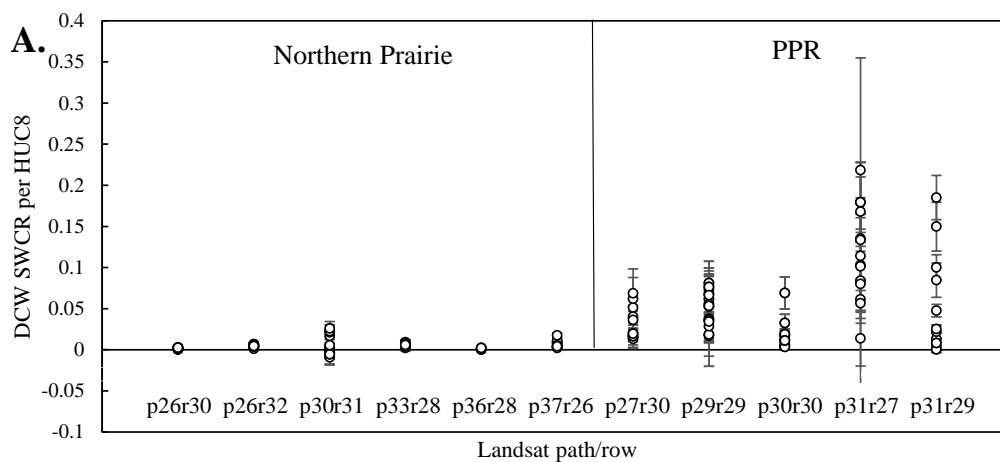
971 **Figure 5.** Examples of minor and substantial expansion of surface-water extent between  
972 historically dry and historically wet points in time. PHDI: Palmer Hydrological Drought Index.



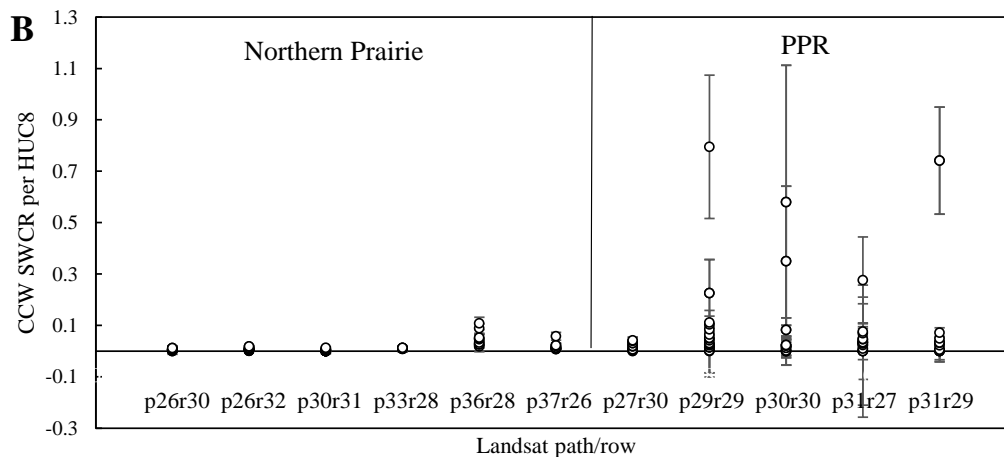
973

974 **Figure 6.** The spatial distribution of the Surface Water Climate Variable (SWCR) values from  
975 the statistical relationships between available water, defined as precipitation minus potential  
976 evapotranspiration accumulated over the previous 9 months, and surface-water extent. Greater  
977 SWCR values indicate greater change in surface-water extent with increased available water.  
978 Surface-water extent was divided between A) disconnected surface water (DCW), or surface-  
979 water extent disconnected from the stream network, and B) continuously connected water  
980 (CCW), or surface-water extent connected to the stream network.

981



982



983

984 **Figure 7.** Distribution of Surface Water Climate Response and standard error values organized  
 985 by Landsat path/row and primary path/row location, i.e., the Northern Prairie or the Prairie  
 986 Pothole Region (PPR) for A) surface water that is disconnected from the stream network (DCW),  
 987 and B) surface water that is connected to the stream network (CCW). HUC8: 8-digit  
 988 Hydrological Units

989

990



991 **Appendix**

992 **Table 1.** A complete list of Landsat TM images used in the analysis and the corresponding  
 993 Palmer Hydrological Drought Index (PHDI).

Landsat path/row	Date	PHDI	Landsat path/row	Date	PHDI	Landsat path/row	Date	PHDI
p26r30	1989 170	-4.29	p30r30	1990 121	-4.70	p31r29	1989 109	-1.62
p26r30	1989 186	-4.29	p30r30	1989 294	-4.66	p31r29	2003 196	-1.22
p26r30	1988 296	-4.15	p30r30	1989 110	-3.47	p31r29	2004 279	2.52
p26r30	1996 222	-0.24	p30r30	1991 236	-2.79	p31r29	1999 121	5.19
p26r30	1987 117	0.06	p30r30	1988 148	-1.23	p31r29	2011 154	6.55
p26r30	1996 142	0.30	p30r30	2002 122	-1.12	p31r29	2010 167	6.94
p26r30	2010 148	1.10	p30r30	2013 184	-0.94	p31r29	2010 279	8.63
p26r30	2006 153	1.17	p30r30	2003 141	0.26	p33r28	1988 249	-5.68
p26r30	2008 95	2.82	p30r30	2003 285	0.88	p33r28	1990 254	-3.87
p26r30	1993 133	3.95	p30r30	1993 161	5.40	p33r28	2008 112	-2.86
p26r30	1993 277	6.92	p30r30	2011 211	6.49	p33r28	1988 137	-2.47
p26r32	1988 264	-4.18	p30r30	2011 179	6.87	p33r28	2005 135	-2.35
p26r32	2000 105	-3.03	p30r30	2010 288	8.93	p33r28	2003 146	-1.78
p26r32	2003 145	-2.98	p30r31	2002 250	-4.62	p33r28	2005 263	-0.62
p26r32	1989 266	-2.92	p30r31	2000 269	-3.75	p33r28	1998 148	0.22
p26r32	1991 288	-1.88	p30r31	2000 173	-2.66	p33r28	2006 106	0.36
p26r32	1991 96	0.55	p30r31	1990 105	-2.63	p33r28	1998 260	0.70
p26r32	2007 108	0.74	p30r31	2003 141	-2.46	p33r28	1995 188	4.09
p26r32	2002 158	1.59	p30r31	1990 297	-2.45	p33r28	1997 129	5.11
p26r32	1994 136	2.76	p30r31	1990 137	-2.43	p33r28	2015 67	5.37
p26r32	1993 133	3.66	p30r31	2003 221	-2.41	p33r28	2014 160	5.61
p26r32	1994 104	3.79	p30r31	2000 221	-2.38	p33r28	2014 256	9.15
p26r32	2010 100	4.06	p30r31	2000 125	-2.05	p36r28	1988 222	-6.07
p26r32	2008 271	5.07	p30r31	2002 122	-1.84	p36r28	2002 212	-5.14
p26r32	2010 228	5.90	p30r31	2005 178	1.58	p36r28	2004 154	-4.72
p27r30	1988 239	-4.52	p30r31	1986 174	2.19	p36r28	2004 282	-4.29
p27r30	1989 161	-4.34	p30r31	1994 148	3.63	p36r28	2003 135	-2.38
p27r30	2003 280	-1.32	p30r31	1994 260	4.12	p36r28	1985 149	-2.04
p27r30	2002 141	-1.25	p30r31	2011 179	5.22	p36r28	1989 112	-1.94
p27r30	2003 104	1.44	p30r31	2009 173	5.29	p36r28	2013 178	-0.91
p27r30	2008 182	3.03	p31r27	1990 160	-4.12	p36r28	1993 91	-0.89
p27r30	1992 266	3.22	p31r27	2006 252	-3.32	p36r28	2013 242	-0.42
p27r30	1992 122	4.29	p31r27	1991 163	-2.45	p36r28	1998 121	1.67
p27r30	1993 172	6.52	p31r27	1992 118	-1.93	p36r28	2008 181	1.70
p29r29	1990 130	-3.55	p31r27	1999 121	2.01	p36r28	1996 244	2.06
p29r29	2003 118	-2.01	p31r27	2007 255	2.41	p36r28	1996 100	3.81
p29r29	2002 323	-1.69	p31r27	1997 195	2.72	p36r28	1993 235	5.17
p29r29	1991 133	-0.69	p31r27	2005 169	3.06	p36r28	1994 142	
p29r29	1992 136	1.35	p31r27	2009 244	3.28	p37r26	1988 213	-5.70
p29r29	2006 286	2.30	p31r27	2004 279	4.38	p37r26	2006 246	-3.41
p29r29	1998 120	2.77	p31r27	2001 190	4.46	p37r26	1994 261	-2.54
p29r29	2005 91	3.15	p31r27	1995 270	5.97	p37r26	2008 108	-2.37
p29r29	2006 94	4.20	p31r27	2010 279	6.43	p37r26	2002 171	-1.85
p29r29	2001 128	4.47	p31r27	2011 186	6.61	p37r26	1991 141	0.14
p29r29	1997 165	5.05	p31r27	1994 299	7.03	p37r26	2009 142	0.26
p29r29	1995 288	5.71	p31r27	2011 266	8.92	p37r26	1995 168	1.35



p29r29	2011	284	5.88	p31r29	2006	172	-3.49	p37r26	1995	264	1.68
p29r29	2010	105	6.19	p31r29	1989	189	-3.38	p37r26	1987	162	2.15
p29r29	1993	266	6.86	p31r29	2004	135	-2.66	p37r26	1991	269	2.26
p29r29	2011	156	8.37	p31r29	1989	269	-2.31	p37r26	1994	101	2.76
p29r29	2010	281	9.63	p31r29	2003	100	-2.24	p37r26	2013	169	3.40
				p31r29	2003	132	-1.84	p37r26	2011	276	7.32
				p31r29	1990	96	-1.65	p37r26	2011	212	9.14

994

995

996